ELSEVIER

Advances in Colloid and Interface Science 133 (2007) 61 – 89

ADVANCES IN COLLOID AND INTERFACE SCIENCE

www.elsevier.com/locate/cis

Review of non-reactive and reactive wetting of liquids on surfaces

Girish Kumar, K. Narayan Prabhu *

Department of Metallurgical and Materials Engineering, National Institute of Technology Karnataka, Surathkal, Srinivasnagar 575025, Karnataka, India

Available online 1 May 2007

Abstract

Wettability is a tendency for a liquid to spread on a solid substrate and is generally measured in terms of the angle (contact angle) between the tangent drawn at the triple point between the three phases (solid, liquid and vapour) and the substrate surface. A liquid spreading on a substrate with no reaction/absorption of the liquid by substrate material is known as non-reactive or inert wetting whereas the wetting process influenced by reaction between the spreading liquid and substrate material is known as reactive wetting. Young's equation gives the equilibrium contact angle in terms of interfacial tensions existing at the three-phase interface. The derivation of Young's equation is made under the assumptions of spreading of non-reactive liquid on an ideal (physically and chemically inert, smooth, homogeneous and rigid) solid, a condition that is rarely met in practical situations. Nevertheless Young's equation is the most fundamental starting point for understanding of the complex field of wetting.

Reliable and reproducible measurements of contact angle from the experiments are important in order to analyze the wetting behaviour. Various methods have been developed over the years to evaluate wettability of a solid by a liquid. Among these, sessile drop and wetting balance techniques are versatile, popular and provide reliable data.

Wetting is affected by large number of factors including liquid properties, substrate properties and system conditions. The effect of these factors on wettability is discussed. Thermodynamic treatment of wetting in inert systems is simple and based on free energy minimization where as that in reactive systems is quite complex. Surface energetics has to be considered while determining the driving force for spreading. Similar is the case of spreading kinetics. Inert systems follow definite flow pattern and in most cases a single function is sufficient to describe the whole kinetics. Theoretical models successfully describe the spreading in inert systems. However, it is difficult to determine the exact mechanism that controls the kinetics since reactive wetting is affected by a number of factors like interfacial reactions, diffusion of constituents, dissolution of the substrate, etc. The quantification of the effect of these interrelated factors on wettability would be useful to build a predictive model of wetting kinetics for reactive systems.
© 2007 Elsevier B.V. All rights reserved.

Keywords: Wetting; Contact angle; Thermodynamics; Kinetics; Modeling

Contents

1. Introduction . . . 62
2. Wettability . . . 63
   2.1. Contact angle . . . 63
   2.2. Types of contact angle . . . 64
   2.3. Contact angle hysteresis . . . 66
   2.4. Measurement of contact angle . . . 68
3. Factors affecting wetting . . . 69
   3.1. Substrate surface roughness . . . 69
   3.2. Heterogeneity of the surface . . . 71
   3.3. Flux . . . 72
   3.4. Temperature . . . 73

* Corresponding author. Tel.: +91 824 2474000x3756; fax: +91 824 2492794.
E-mail address: prabhukn_2002@yahoo.co.in (K.N. Prabhu).

0001-8686/$ - see front matter © 2007 Elsevier B.V. All rights reserved.
doi:10.1016/j.cis.2007.04.009

3.5. Trace elements . . . 74
3.6. Atmosphere . . . 76
3.7. Liquid properties . . . 76
4. Thermodynamics of wetting . . . 77
4.1. Inert systems . . . 77
4.2. Reactive systems . . . 78
5. Kinetics of wetting . . . 79
5.1. Inert systems . . . 81
5.2. Reactive systems . . . 81
6. Modeling of spreading . . . 82
6.1. Model for complete spreading . . . 83
6.2. The hydrodynamic model . . . 83
6.3. The molecular kinetic model . . . 84
6.4. Combined models . . . 84
6.5. Frenkel's approach . . . 85
6.6. Overall energy balance approach . . . 85
6.7. Model for spreading on rough surface . . . 85
6.8. Models for spreading in reactive systems . . . 86
7. Summary . . . 87
References . . . 88

1. Introduction

The process of wetting a solid by a liquid is of great technological importance. A large number of general/biological/industrial/manufacturing/fabrication processes essentially involve wetting phenomenon [1,2]. Printing, painting, adhesion, lubrication, cleaning, coating, soldering, brazing and composite processing are few examples among the innumerable fields utilizing the phenomenon of wetting. Some applications require a good wetting between liquid and substrate surface whereas some others demand poor wetting or repellency. Consider the process of soldering, for example, which is a metallurgical joining method that uses a filler metal known as solder to hold the parts to be joined together. The basic soldering process depends on wetting for the formation of solder-to-base metal contact. The solidification of molten solder after wetting results in permanent bond. Therefore, the solderable surfaces must allow the molten solder to wet and spread within the available time [3,4]. On the other hand, the well known "lotus effect" of plant surfaces towards water plays a vital role in self cleaning mechanism [5,6]. The removal of contaminating particles from plant surfaces is achieved by rolling water droplets which do not stick to the surface. Using the same idea ultra or super hydrophobic surfaces have been developed which give water contact angles as high as 160° or more.

Wetting of a solid by a liquid is a surface phenomenon in which the surface of the solid is covered by the liquid on placing it over the surface. Spreading is a physical process through which liquid wets the surface. It can be defined as the increase in the area of coverage by the liquid with respect to time on placing a drop of liquid on the surface. For example, consider a drop of liquid placed on a solid substrate as shown in Fig. 1(a)–(c). Fig. 1(a) represents the drop at time, $t=0$ s or at the moment when the drop is placed on the substrate. The successive figures show the spreading of liquid drop at increased time periods. The continuous decrease in the contact angle and continuous increase of the base diameter as well as contact area are common features of spreading of a liquid on a solid.

Wetting or spreading can be broadly classified into two categories, viz., non-reactive wetting and reactive wetting. A liquid spreading on a substrate with no reaction/absorption of the liquid by substrate material is known as non-reactive or inert wetting. On the other hand, the wetting process influenced by reaction between the spreading liquid and substrate material is known as reactive wetting. Spreading of water or polymeric liquids on glass or metallic substrate is an example of non-reactive wetting where as the wetting ceramic substrate by a liquid metal and spreading of solder on copper substrate are few examples of reactive wetting. Alteration of interface and formation of intermetallic compounds are the two important features of reactive wetting. Fig. 2 is a sketch of a solder/substrate interface where the reactive wetting process resulted in the formation of intermetallic compounds.

Spreading of most of the non-metallic liquids on inert solids is generally non-reactive type. The whole process is spontaneous and almost completes within small duration of time. This phenomenon is governed by capillary/surface tension, gravity and viscous forces in the order given. On the other hand, spreading of metallic liquids on solid substrates is guided by additional factors such as diffusion, reaction, absorption, solidification, etc. The true equilibrium state is rarely achieved in such systems.

The other way to classify the spreading is on the basis – how the process is initiated and driven. There are two types – spontaneous spreading and forced spreading [8]. A liquid drop

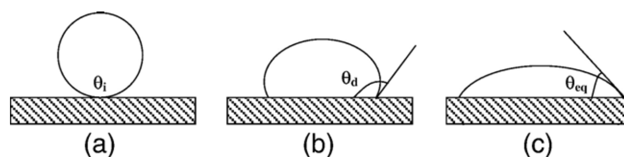

Fig. 1. (a)–(c) Spreading drop of liquid on a solid substrate.

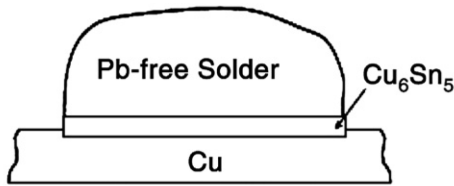

Fig. 2. Schematic sketch of a solder/substrate interface [7].

spreading on the solid by itself without any external interference is termed as spontaneous spreading and forced spreading otherwise. Spreading of solder paste during reflow soldering is a classic example of spontaneous spreading. The spreading of water drop after impacting from a finite height is forced spreading since the spreading drop gains considerable kinetic energy during its fall which drives spreading initially. Both of these processes have numerous industrial applications and hence investigated in great detail [4–6,8].

In this review, the wetting behaviour in inert and reactive systems are compared. First, the concepts of wettability and contact angle are introduced. This is followed by a discussion on the factors affecting the evolution of contact angle. The thermodynamics and kinetics of wetting in both systems are dealt subsequently. The methods and difficulties associated with the measurement of wettability are highlighted. Theoretical and empirical models available for modeling of spreading behaviour are presented for both types of systems.

2. Wettability

Wettability can be defined as the tendency for a liquid to spread on a solid substrate [9]. It describes the extent of intimate contact between a liquid and a solid [10]. There are two important parameters to characterize the wettability of a liquid on a solid [4,11]. They are:

- Degree or extent of wetting, and
- Rate of wetting.

The degree of wetting is generally indicated by the contact angle formed at the interface between solid and liquid. In the equilibrium case, it is governed by the laws of thermodynamics. It is dependent on the surface and interfacial energies involved at the solid/liquid interface. The rate of wetting indicates that how fast the liquid wets the surface and spreads over the same. It is guided by number of factors such as the thermal conditions of the system, capillary forces, viscosity of the liquid, the chemical reactions occurring at the interface, etc.

Whenever a drop of liquid is placed on a solid substrate surface any of the following phenomena may take place either alone or in combination depending on the properties of the spreading liquid and/or substrate, system/environmental conditions, etc.

- The drop of liquid may spread continuously to cover the whole substrate surface completely by a thin film. This is generally known as complete wetting.
- The liquid drop may spread partially to some extent and come to rest within a short period of time—a case generally referred as partial or incomplete spreading.
- The liquid may spread a little or may not spread at all. A highly lyophobic surface such as the behaviour of lotus leaf against water shows this type of behaviour.
- The spreading liquid may stop its movement due to solidification.
- The liquid may evaporate over a period of time. This generally takes place in case of volatile liquids or when water is placed on a heated surface.
- The spreading liquid may be consumed by the substrate by chemical reaction/diffusion—the phenomenon of reactive wetting.
- The liquid may get adsorbed and subsequently absorbed by the substrate. Porous substrates generally behave in this manner.

These possibilities clearly indicate the complexity of the wetting process and forces responsible for the happening of the above. Each of the above phenomena has its own biological and/or technological importance. For example, super-hydrophobic surfaces are very useful in cleaning activities where as reactive spreading is responsible for the bond formation in soldering and brazing. Similarly evaporation of the spreading liquid finds application in quenching operations involved in industrial heat treatment [12–14].

In the simplest case of spreading of a non-reactive liquid on smooth and inert solid only surface tension and viscous forces act upon and determine the equilibrium state. However, the real situation is quite complex as already pointed out and a great number of factors affect the process and in most cases do not allow the equilibrium to achieve.

2.1. Contact angle

When a liquid sits on a solid surface, it will spread to some extent on the surface and then comes to rest making an angle with it as shown in the Fig. 3. The angle between the tangent drawn at the triple point between the three phases (solid, liquid and vapour) and the substrate surface is known as contact angle. Under equilibrium conditions this angle is decided by the surface and interfacial energies. Contact angle has been widely used for characterizing interfacial phenomena, wetting/dewetting of solid surfaces, capillary penetration into porous media, coating, painting, etc. [15,16].

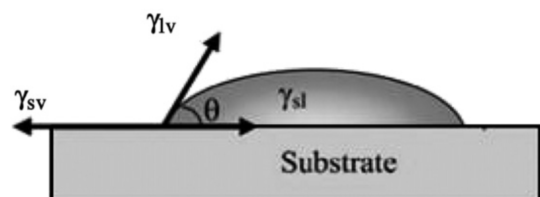

Fig. 3. Sessile drop on a solid substrate.

Consider a pure liquid wetting and spreading on an ideal surface i.e., a smooth surface of an inert solid. Under these conditions, the dynamic driving force for wetting ($F_d(t)$) is given by:

$$F_d(t) = \gamma_{sv} - (\gamma_{sl} + \gamma_{lv}\cos\theta(t)) \quad (1)$$

where γab is the interfacial tension between the phases a and b and subscripts s, l, v indicate the solid, liquid and vapour phases respectively.

At equilibrium, the spreading ceases and drop comes to rest. Hence, there is no driving force for spreading or $F_d=0$. This condition results in Young's equation [17,18]:

$$\gamma_{sv} - \gamma_{sl} = \gamma_{lv}\cos\theta \quad (2)$$

Dupre defined the work of adhesion between solid and liquid as follows [19]:

$$W_{sl} = \gamma_{sv} + \gamma_{lv} - \gamma_{sl} \quad (3)$$

Insertion of Eq. (3) in Eq. (1) yields famous Young–Dupre equation:

$$W_{sl} = \gamma_{lv}(1 + \cos\theta) \quad (4)$$

For a given value of γ_{lv}, the contact angle increases as the adhesion between the liquid and solid decreases. An angle of 180° indicates zero adhesion between the liquid and surface and therefore represents a total non-wetting condition. Under this condition, ($\gamma_{sl}-\gamma_{sv}$) is larger than γ_{lv} and the drop is in a pure drying situation [20]. It is very difficult to achieve such a situation physically. But, inversion of liquid and vapour phases will make it possible. That is, a bubble of air rising in a box filled with oil reaches the top of the box with a contact angle of 180°. For practical purposes, the liquid is said to wet the surface of solid when the contact angle is less than 90°. On the other hand, if the contact angle is greater than 90°, the liquid is considered as non-wetting the solid. In such cases, the liquid drops tend to move about easily on the substrate surface and do not have any tendency to enter into pores or holes by capillary action. It is generally accepted that the smaller the contact angle, the better the wettability. Hence, good wettability can be expected when γ_{lv} is as large as possible while γ_{sv} and γ_{sl} are as small as possible [21].

The liquid is considered to wet the solid completely only when the contact angle is zero. This is the case when ($\gamma_{sv}-\gamma_{sl}$) is larger than γ_{lv} [20]. Hence, the drop tends to spread completely on the solid. There are many systems showing such behaviours. For example, silicone oil completely wets most of the solids like glass, steel, plastics, etc. However, when θ is zero, Young's equation ceases to hold and the imbalance of surface free energies is given by spreading coefficient, S, defined as follows [15]:

$$S = \gamma_{sv} - (\gamma_{sl} + \gamma_{lv}) = \gamma_{lv}(\cos\theta - 1) \quad (5)$$

The distinction between different states can be made with the help of spreading coefficient defined above. It is negative for partial wetting state since the sum of solid/liquid and liquid/vapour interfacial tensions is greater than the solid/vapour tension and hence, it is unfavourable to replace the solid/vapour interface. On the other hand, for complete wetting the spreading coefficient is zero or positive [22]. At the limiting case, solid/vapour interfacial tension is equal to the sum of solid/liquid and liquid/vapour interfacial tensions. As a result, the solid/vapour interface is not stable or does not exist.

Fig. 4 schematically shows a liquid drop on a solid substrate under various different conditions: from complete wetting ($\theta=0°$) to total non-wetting condition ($\theta=180°$).

The work of adhesion can be thought as the work that must be performed per unit area of the interface to separate the two phases. Hence, it is a measure of strength of binding between the phases. A lower value of contact angle indicates better adhesion. For complete wetting, $\theta=0°$, which corresponds to $W_a=2\gamma_{lv}$ and this gives the condition for perfect wetting as $W_a\geq 2\gamma_{lv}$. Further this value of adhesion energy is nothing but the work of cohesion or the energy spent on keeping the two phases together.

The derivations of Young's as well as Young–Dupre equations are made under the assumptions of spreading of non-reactive liquid on an ideal (physically and chemically inert, smooth, homogeneous and rigid) solid. Further it is also assumed that the contact angles are large enough to allow accurate measurement [24]. The condition is rarely met in the practical situations. However, Young's equation is the most fundamental starting point for understanding of the complex field of wetting.

2.2. Types of contact angle

The process of wetting and spreading involves the flow of fluid over the surface of a solid. This flow is affected by number of factors such as viscosity of fluid, roughness and heterogeneity of the surface, temperature of the fluid as well as the substrate, quantity or volume of fluid spreading, reaction between the fluid and surface of substrate, etc. Hence, it is difficult to find a reproducible contact angle in any system as the number of system parameters or variables are too large to control. As a result, a large scatter is found amongst the contact angles reported by various researchers. For example, let us look into the

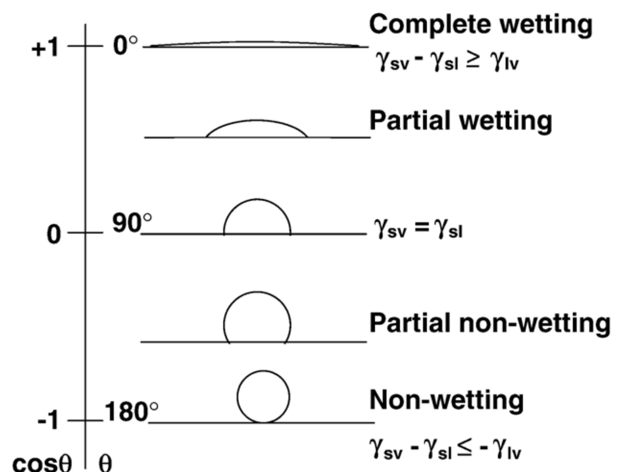

Fig. 4. Liquid drop on a solid substrate under various wetting conditions [23].

contact angles reported in the literature for various solder/substrate systems. Bhukat et al. [25] reported a contact angle of 70° for a lead–free Sn–3.5Ag solder on a Cu substrate where as Takao et al. [26] found it around 43° on bare Cu plate and 29° on Au plated Cu. Hong et al. [27] gives a range of values for the wetting of Sn–3.5Ag solder on Au metallized Cu plates from 27° to 67° depending on the type of flux used. A value of 34.2° is reported for equilibrium contact angle for the same solder on Cu plate in an inert atmosphere by Mackie [28]. Table 1 gives the values of contact angles for various solder/substrate systems reported in literature.

Table 1
Contact angle data reported in the literature

Solder/substrate	Condition	Contact angle	Ref.
Sn–37Pb/Cu	260 °C	17	[9]
Sn–3.5Ag/Cu	260 °C	36	
Sn–5Sb/Cu	280 °C	43	
Sn–58Bi/Cu	195 °C	43	
Sn–50In/Cu	215, 230, 245 °C RMA [a] flux is used in all cases	63, 41, 33	
Sn–3.5Ag/Cu	250, 270 °C	70, 50	[25]
Sn–3Ag–0.5Cu/Cu		55,–	
Sn–3.6Ag–0.7Cu/Cu		55, 40	
Sn–4Ag–0.5Cu/Cu		55, 40	
Sn–2.5Ag–1Bi–0.5Cu/Cu		55, 52	
Sn–2.5Ag–0.7Cu/Cu	*x*=0, 0.1, 0.25%	53	[29]
Sn–3.5Ag–0.7Cu–*x*RE/Cu		48, 41, 46	
Sn–37Pb/Cu	–	10	[30]
Sn–4Ag–0.5Cu/Cu		30	
Sn–37Pb/Cu–Ni–Au		7	
Sn–4Ag–0.5Cu/Cu–Ni–Au		27	
Sn–37Pb/UBM–1,2,3,4 [b]	–	61, 10, 64, 62	[27]
Sn–3.5Ag/UBM–1,2,3,4 [b]		64, 27, 67, 60	
Sn–3Ag–*x*Bi/	250 °C	70–85	[31]
Fe–42Ni	450 °C *x*=0, 3 and 6%	50–65	
Sn–9Zn–*x*Cu/Cu	Cu=0, 0.5, 1, 2, 4, 6, 8, 10%	Cu=0, 0.5, 1, 2, 4, 6, 8, 10%	[32]
Sn–37Pb/Cu	250 °C	13–32	[33]
Sn–3.5Ag–*x*Cu/Cu	250 °C – 280 °C *x*=0, 0.5, 0.75% Different types flux and surface roughness	28–55	
60Sn–In–*x*Bi/Cu	272 °C (*x*=5, 10, 20, 40%)	25, 21, 19, 15	[21]
Sn–37Pb/Cu	270 °C	23	[26]
Sn–3.5Ag/Cu		43	
Sn–3.5Ag/Cu	Halide-free flux	43	[26]
Sn–3.5Ag/Cu	Halide flux	38	
Sn–3.5Ag/Cu	1% Cu	42	[26]
Sn–3.5Ag/Cu	5% In	41	
Sn–3.5Ag/Cu	5% Bi	38	
Sn–3.5Ag/Cu	1% Zn	48	
Sn–3.5Ag/Cu	Au plated	29	[26]
Sn–37Pb/Cu	–	11.1	[28]
Sn–0.5Cu/Cu		33.9	
Sn–3.5Ag/Cu		34.2	
Sn–0.7Cu–*x*Zn/Cu	*x*=0, 0.2, 0.6 and 1%	42, 46, 52 and 50	[34]

[a] RMA: Rosin mildly activated.
[b] UBM 1: Au(500 Å)/Cu(1000 Å)/Cr(700 Å). UBM 2: Cu(5000 Å)/Cr (700 Å). UBM 3: Au(500 Å)/Cu(5000 Å)/Cr(700 Å). UBM 1: Au(500 Å)/Cr (1000 Å)/Ti(700 Å).

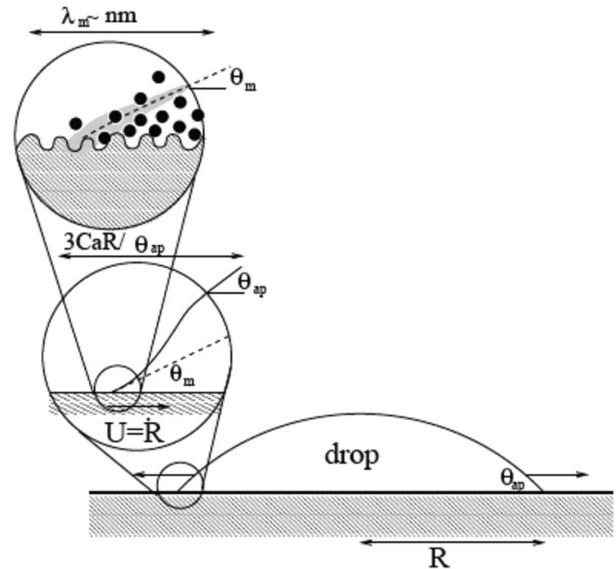

Fig. 5. Contact angle at macro and micro scales [37].

A close examination of the contact angles mentioned in the literature implies that the scatter could be the consequence of sensitivity of contact angle to various factors specific for the spreading liquid, substrate, atmosphere, etc. A variety of contact angles has been defined to address different situations [12]. Contact angle formed at the 3-phase interface under equilibrium conditions during the wetting of an ideal solid surface by a non-reactive liquid is generally termed as equilibrium contact angle. The equilibrium contact angle formed under the situations where no oxide or any other film/contaminant covering the substrate surface or spreading liquid is termed as intrinsic contact angle. It can also be defined as the contact angle at the molecular distance from the solid surface [35]. The contact angle determined by balancing the surface tension forces is known as Young's contact angle. It is the single contact angle predicted by Young's equation (Eq. (2)) for an ideal (smooth, homogeneous, rigid and insoluble) surface under thermodynamic equilibrium conditions. However, a range of contact angles has been observed to form on real solid surface. The contact angle obtained when a liquid drop is placed on real surface is known as apparent contact angle. Marmur defined apparent contact angle as the macroscopic angle formed at the 3-phase boundary where the tangent is drawn to the nominal

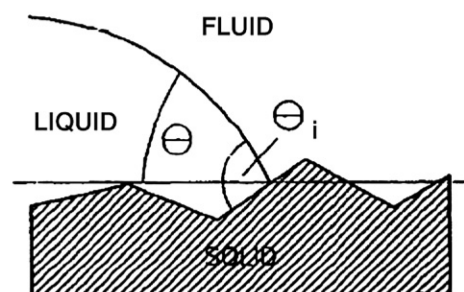

Fig. 6. Apparent and intrinsic contact angle [35,36].

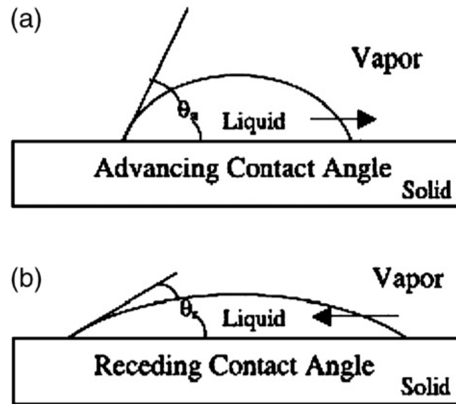

Fig. 7. (a), (b) Advancing and receding contact angles [38].

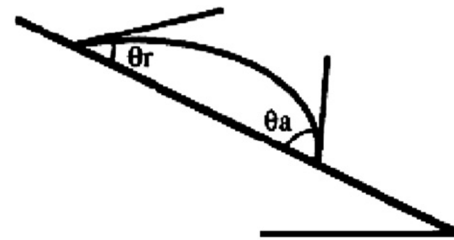

Fig. 8. Drop on a tilted substrate [39].

surface with such a magnification that the details of the roughness of the surface is not observed [35,36]. Fig. 5 shows how apparent contact can be different from the intrinsic contact angle formed at the true interface during the spreading of a drop. The apparent contact angle obtained on a rough but homogeneous surface is generally referred as Wenzel angle and that obtained on a smooth but heterogeneous surface is known as Composite contact angle or Cassie angle. Fig. 6 is a schematic representation of a drop on a geometrically rough surface where a clear distinction can be made between the Wenzel's apparent angle and true intrinsic angle.

All the above angles are classified as static contact angles since the determination of contact angle is done after drop spreading has ceased. On the other hand contact angles determined while the contact line is still moving is known as dynamic contact angle. The contact angle determined when the interface is advancing towards the vapour phase is known as advancing contact angle where as the contact angle determined when the interface is moving away from the vapour phase is known as receding contact angle. In many systems the true equilibrium static contact angle rarely attains. In such situations the contact angle is determined at a point when its change is negligibly small or when the system reaches a metastable state and this contact angle is known as quasi-equilibrium contact angle. Fig. 7 represents the advancing and receding contact angles. Table 2 gives the definitions of various contact angles reported in the literature.

Table 2
Types of contact angles

S. No.	Contact angle	Definition
1.	Intrinsic	The contact angle made by the liquid with an ideal (rigid, flat, smooth, homogeneous, insoluble and non-reactive) solid surface.
2.	Equilibrium, Young's	Contact angle obtained by equating the surface tension forces. $\theta=\cos^{-1}[(\gamma_{sv}-\gamma_{sl})/\gamma_{lv}]$
3.	Wenzel	Apparent contact angle obtained on a rough and homogeneous surface. $\theta_w=\cos^{-1}[r\cos\theta]$
4.	Composite (Cassie)	Contact angle obtained on a smooth composite surface $\theta_c=\cos^{-1}[f_1\cos\theta_1+f_2\cos\theta_2]$
5.	Apparent contact angle	Contact angle obtained on a real surface
6.	Dynamic, instantaneous	Time dependent contact angle
7.	Advancing	The contact angle determined when the interface is advancing toward the vapour phase
8.	Receding	The contact angle determined when the interface is receding away from the vapour phase

2.3. Contact angle hysteresis

The Young's equation is valid only for smooth, homogeneous, isotropic and non-deformable surfaces. For real surfaces, a range of contact angles exists along the contact line of a static drop. The largest and the smallest among them are generally termed as the advancing and the receding contact angles respectively [5,16,18,20]. This phenomenon of existence of multiple contact angles for a single drop is known as hysteresis of contact angle. The advancing contact angle is generally measured for a liquid advancing across the surface of a solid where as the receding contact angle is measured for the liquid receding from the surface. It is observed that advancing contact angle exceeds the receding one and this difference is known as contact angle hysteresis [22]. A drop usually sticks to the solid, even if it is tilted, due to contact angle hysteresis. In such a situation, the contact angle at the rear is given by $\theta_r=\theta_m-(\Delta\theta/2)$ where as the contact angle at the front is $\theta_a=\theta_m+(\Delta\theta/2)$. Here $\Delta\theta$ is the contact angle hysteresis and θ_m is the mean

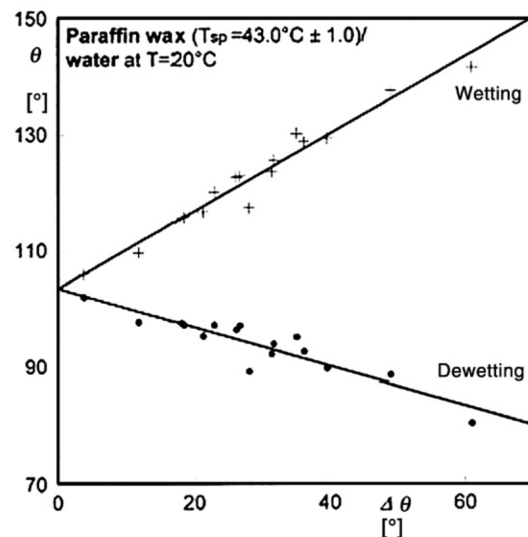

Fig. 9. Experiment of wetting/dewetting of water on paraffin wax surface [40].

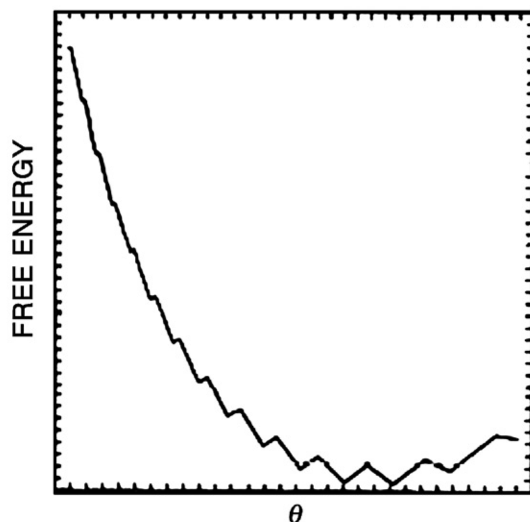

Fig. 10. A typical free energy curve exhibiting multiple metastable states [35,36].

contact angle. Fig. 8 schematically shows how advancing contact angle differs from a receding one for a drop on tilted substrate and the existence of contact angle hysteresis.

Hysteresis is a general phenomenon observed in number of practical situations. Examples include magnetic, dielectric and mechanical hysteresis. The existence of domains exhibiting irreversible transition between the states is cited to be the reason for the occurrence of hysteresis phenomenon. The Contact angle hysteresis could be due to substrate surface roughness and heterogeneity, impurities adsorbing on to the surface, swelling of the surface (generally takes place on polymer surfaces), rearrangement or attraction of the surface by the solvent, etc. [15,16,40]. It is generally observed that cleaner the surface, smaller the contact angle hysteresis. According to Davis et al., the advancing contact angle is due to a film which prevents the liquid from adhering to the surface [19]. However, once the surface comes into contact with the liquid, the film may be removed either partially or wholly so that more complete contact between the liquid and the solid takes place. As a result, the system gives smaller receding contact angles and this difference in advancing and receding contact angles gives rise to hysteresis.

Two different effects occur in wetting on a rough and chemically homogeneous solid [40]. They are: (i) the barrier effect and (ii) the capillary attraction/depression. The increase in contact angle hysteresis with growing roughness is known as the barrier effect. Further, advancing contact angle (θ_a) increases by the same amount as receding contact angle (θ_r) decreases with growing roughness due to the barrier effect. Hence, for a pure barrier effect equilibrium contact angle (θ_e) is given by: $\theta_e = 0.5(\theta_a + \theta_r)$.

As a result of capillary attraction or depression of grooves in the surface, for $\theta_e < 90°$, wettability improves with increasing roughness. On the other hand, for $\theta_e > 90°$, wettability will be worse on a rough surface than on a corresponding smooth surface. It is reported that, capillary effect causes an increase in both advancing and receding contact angles with growing roughness for $\theta_e < 90°$ and an opposite effect is observed if $\theta_e > 90°$. Only at $\theta_e = 90°$, capillary has no effect.

Kamusewitz et al. proposed an empirical relation connecting contact angle hysteresis and advancing or receding contact angle with equilibrium contact angle with an assumption that truly smooth surface does not give any hysteresis [40]. By plotting advancing or receding contact angle as a function of contact angle hysteresis and extrapolating it to zero hysteresis it is possible to determine equilibrium contact angle. The validity of the proposed empirical relation was successfully checked with number of non-reactive systems like DI water/wax, diethylene glycol/wax, etc. Fig. 9 shows the results of their experiment of wetting/dewetting of water on paraffin wax surface.

Texturing of a solid modifies the contact angle hysteresis and it also affects the mean contact angle [20]. Gaydos and Newmann experimentally determined the minimum patch size i.e., patterned surface or the surface with vertical strips of alternating surface energy, necessary to cause contact angle hysteresis and reported a large value of about 1 μm [19].

A system is considered to exhibit hysteresis if the independent variable has a multibranched non-linearity relation with

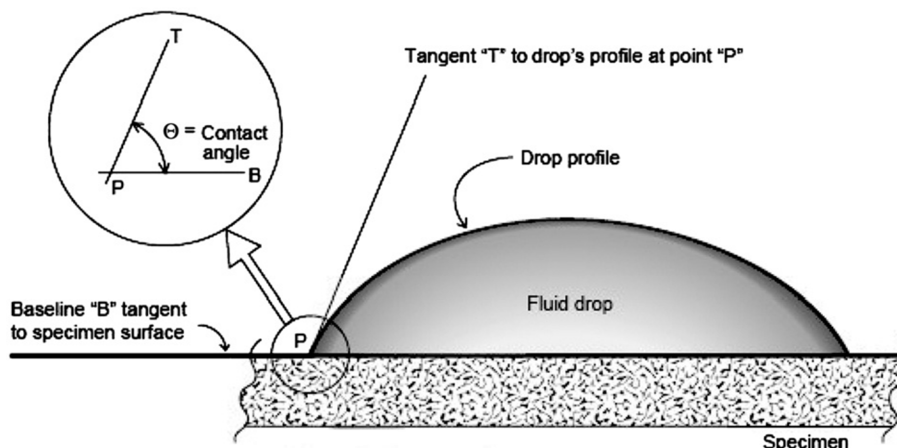

Fig. 11. Sessile drop technique of contact angle measurement [43].

dependent variable [35,36]. The presence of a multivalued property of a system implies the existence of metastable equilibrium states. A typical free energy curve exhibiting multiple metastable states is shown in Fig. 10. A drop remains in a metastable state if it does not possess energy needed for overcoming the barrier between the state and the next one in the direction of stable equilibrium.

2.4. Measurement of contact angle

The wettability measurement has an important role in wetting studies. Reliable and reproducible contact angle value should be available from the experiments in order to analyze the behaviour. Various methods have been developed over the years to evaluate wettability of a solid by a liquid. Among these, sessile drop and wetting balance techniques are versatile, popular and provide reliable data. The two tests are complementary to each other. Each of the tests involves a balancing of surface tensions at a three-phase junction [4,41]. A brief description of these methods is given here.

The method of parallel plates involves measuring the meniscus rise of the liquid between the parallel plates. The dip test is commonly used to assess the wettability of solders. In this test, the component is prefluxed and heated to a predetermined temperature prior to dipping into a solder bath. The bath is kept at constant temperature. The component is immersed at a known rate, held for a known time and withdrawn at a known rate. Then the component is visually inspected to assess the amount of solder adhered to the surface. Though the method is simple it is not reliable as it does not provide any numerical parameters and depends on qualitative judgment.

Sessile drop technique of measuring the contact angle is used by a large number of researchers [4,17,33,42] since it simulates the actual conditions in many applications. For example, the method as applicable to solder drops on a substrate is a simulation of reflow soldering process. However, a large scatter is found in the data reported in the literature and these inconsistencies in the wetting behaviour can be attributed to the purity of the atmosphere, physical conditions of the wetting system employed during the experiments [10]. In this test, a known quantity of liquid is placed on the substrate and allowed to spread. The images of a spreading sessile drop are captured and processed (Fig. 11). Contact angles are measured by fitting a mathematical expression to the shape of the drop and then calculating the slope of the tangent to the drop at the solid–liquid–vapour interface. The principal assumptions in drop shape analysis are:

- The drop is symmetric about a central vertical axis.
- The drop is not in motion. That is, only interfacial tension and gravity are the forces shaping the drop.

The area of spread, the height of the drop from the substrate surface, etc. can also be used to evaluate wettability. The area of spread, contact angle and drop height are geometrically interrelated for any axisymmetric drops and any one parameter may be calculated if the other two are known.

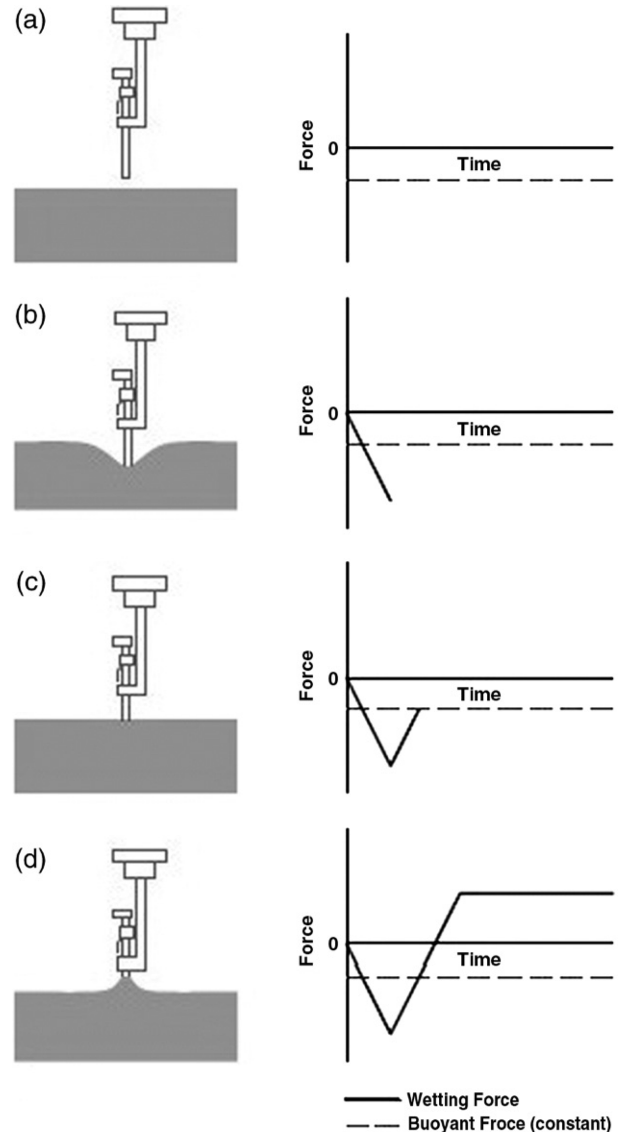

Fig. 12. Wetting balance technique of contact angle measurement [41].

A number of researchers followed wetting balance or tensiometer method to evaluate wettability [44–48]. The wetting balance was basically developed to test the solderability of components leads in a wave soldering process [41]. The balance measures the force produced by the liquid meniscus when a solid test specimen is partially immersed into a liquid. This force is plotted as a function of time to generate the wetting curve and compared with standard curve (Fig. 12).

Awasthi et al. suggested a method for measuring the contact angle of liquid metals which utilizes the property of forming a mirror surface (convex/concave) when contained in a small cup [49]. The radius of curvature of the surface of the liquid metal (R) is determined by ray tracing technique. Knowing this data and the diameter of the cup (D), the contact angle can be determined by using the relation:

$$\theta = \cos^{-1}\left(\frac{-D}{2R}\right) \tag{6}$$

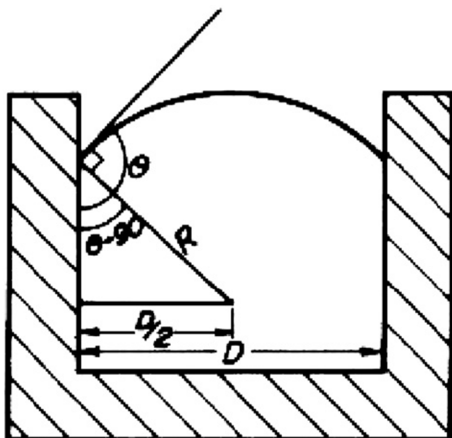

Fig. 13. Geometry of the cup [49].

They applied the above method successfully to determine the contact angle of mercury with graphite. The geometry of the cup is shown in Fig. 13.

3. Factors affecting wetting

Wetting of solid by a liquid is a complex phenomenon sensitive to large number of factors. Non-reactive wetting is generally affected by materials of spreading liquid and substrate (i.e., wetting system), roughness and heterogeneity of the surface, physical properties of the spreading liquid and atmospheric conditions. On the other hand, reactive wetting process is affected by some more factors such as flux usage, trace impurity addition, etc., in addition to the above. The important factors that affect the wetting behaviour of a liquid on a solid are briefly discussed below [50].

3.1. Substrate surface roughness

Rough surfaces have a significant influence on the wetting behaviour of fluids. Fig. 14 is a schematic representation of sessile drop on smooth (Fig. 14(a)) and rough (Fig. 14(b)) surface. It is evident that a rough surface provides an additional interfacial area for the spreading liquid and the true contact angle would be different than the nominal contact angle. The additional surface area provided by roughening the surface results in the increase of surface energy. Wenzel studied the effect of surface roughness on the equilibrium contact angle and proposed an equation that gives a relation between equilibrium contact angle and the apparent angle formed on a rough surface [15,18,33,42,51,52].

$$\cos\theta_{\mathrm{w}} = r\ \cos\theta \tag{7}$$

where θ is the equilibrium contact angle, θ_{w} is the apparent contact angle on a rough surface (generally known as Wenzel angle) and r is the average roughness ratio, the factor by which roughness increases the solid–liquid interfacial area. Hence r is the ratio of actual wetted surface area to projected or geometric surface area calculated from radius of wetted base. Its value is always greater than unity except for ideally smooth surfaces for which it becomes equal to unity.

The physical interpretation of the equation indicates that:

For contact angles less than 90°, apparent contact angle decreases with increase in roughness. On the other hand, apparent contact angle tend to increase with increasing roughness for contact angles greater than 90°. In other words, both lyophilicity and lyophobicity are reinforced by roughness [5,53].

According to Shuttleworth et al. local distortion of contact line on rough surface results in a number of micro contact angles [54]. They proposed the expression:

$$\theta_{\mathrm{r}} = \theta \pm \alpha \tag{8}$$

for apparent contact angle, θ_{r}. Here, α is the maximum angle of the local surface which can either be positive or negative. Fig. 15 depicts a situation in which distorted contact surface can be seen. Hitchcock et al. [56] experimentally investigated the effect of roughness on wetting to compare the models of Wenzel and Shuttleworth. They observed that:

$$r = 1 + C_1(R/\lambda)^2 \tag{9}$$

$$\alpha = \tan^{-1}(C_2R/\lambda) \tag{10}$$

where r is the Wenzel's roughness factor, α is the local surface tilt angle with nominal surface, R is the RMS surface height and λ is the average distance between the asperities of the rough surface.

In non-reactive systems like spreading of non-metallic liquids on inert substrates the role of roughness is limited to

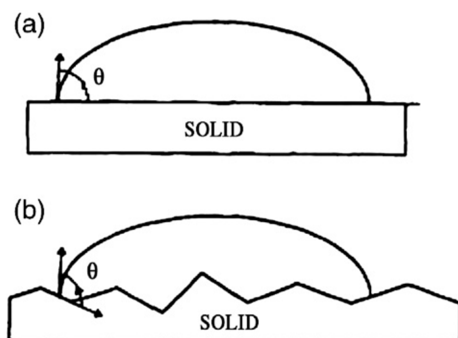

Fig. 14. Sessile drop on smooth and rough surface [35,36].

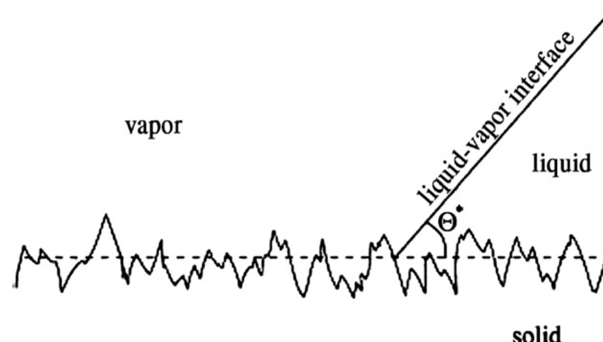

Fig. 15. Distortion of a local surface [55].

alteration of interfacial area and thereby changing the value of surface free energy associated with interface. At extreme values it may hinder the spreading process by providing metastable states due to physical dimensions or by entrapping air/vapour thereby producing a composite surface as observed by some researchers [38]. On the other hand, in reactive systems, the roughness has additional effects. The asperities and grooves may act as preferable sites for reaction, diffusion, adsorption, nucleation, etc. Hence, it would be difficult to assess the effect of roughness alone on wetting behaviour of metallic liquids as the main effects are masked by other factors.

Cazabat and Stuart studied the spreading of non-volatile liquids on rough surfaces [57]. They observed that the prediction of wetting kinetics is based on the assumption that the surface is ideally smooth. Glass substrates in the roughness range 2 μm–50 μm were used in their investigations on the wetting of those surfaces by silicone oils of three different viscosities (0.02, 0.1 and 1 Pa s). Spreading on a smooth surface generally consists of two regimes, viz. capillary and gravity. On the other hand, the spreading on a rough surface is characterized by an additional regime where liquid spreads quickly in the roughness of the surface till it is consumed by troughs and valleys on the surface.

Volpe et al. carried out wetting experiments on smooth and rough heterogeneous surfaces prepared on glass slides by organic liquids [58]. The advancing and receding contact angles were measured and plotted against contact angle hysteresis. By extrapolating the contact angle variation curve to zero hysteresis, equilibrium contact angle was obtained. However, their observation contradicts the Wenzel's result.

Kandlikar and Steinke observed interface behaviour during boiling of DI water on copper and stainless steel substrates to investigate the effect of surface roughness and surface temperature on dynamic contact angle using a photographic technique [38]. Their experiments yielded interesting results. The highest contact angle was obtained with smoothest surface in all cases. The contact angle decreased with increasing surface roughness up to a critical value of roughness. Further increase in roughness resulted in the increase in contact angle (Fig. 16).

Sikalo et al. reported an opposite trend in their investigations on the impact of droplets on horizontal surface [59]. Glass target surfaces of smooth (R_a=0.003 μm) and rough (R_a=3.6 μm) topography were used to receive droplets of water, isopropanol and glycerin impacting from varying heights. The contact angle of isopropanol on glass was reported as zero on surfaces of either roughness as high spreading as well as evaporation rate prevented from any meaningful static contact angle. The wettability of glass decreased significantly on a rough topography when water impacted on the surface. The advancing contact angle on the smooth surface was determined as 10° where as on the rough surface the corresponding value was 78°. The maximum spread and spreading rate for the rough glass were lower than those for the smooth surface. These results are completely opposite of the wetting behaviour generally observed. One possibility is that the roughness measure of the rough glass surface could be higher than the critical value. However, this could not be verified since experiments on intermediate roughness glass surfaces were not carried out.

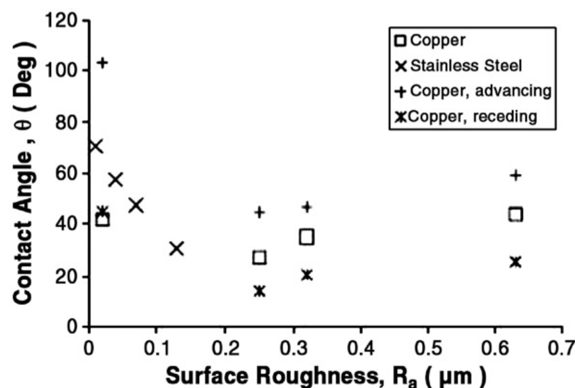

Fig. 16. Contact angle as function of roughness as investigated by Kandlikar [38].

It has been shown by Li et al. that plasma treatment could change the surface roughness and hence wettability of polymer surfaces [60]. Experiments were carried out to investigate the improvement in adhesion between gold thin film and a polymer by utilizing pure Ar, O_2 and 2:1 mixture of O_2/CF_4 as processing gases for plasma treatment keeping other parameters constant. The surface topography of the polymer surface was studied before and after the treatment by using field emission scanning electron microscope. The FESEM (Field emission scanning electron microscope) images clearly showed the change in surface roughness and topography after plasma treatment particularly when O_2/CF_4 was used as processing gas. The contact angle between water and treated polymer surface was measured to determine if there is a change in wettability. The Ar plasma treatment resulted in the contact angle relaxation from initial 81° to 50° within 2 min and the drop stabilized where as the O_2 plasma performed even better. The contact angle reduced from 81° to 14° within 5 min before stabilization. The treatment of the surface by O_2/CF_4 plasma resulted in excellent improvement in wettability as the surface turned to completely wettable. The contact angle relaxed to almost zero within a minute after dispensing the drop.

Solid surfaces become hydrophilic when irradiated by plasma since the gas adsorption layer is removed by plasma and an active oxide layer appears on the surface as suggested by Takata et al. [61]. The surfaces of copper, aluminium and stainless steel were polished to different surface finish conditions and then subjected plasma irradiation. Water contact angles were measured to study the effect of plasma treatment. A significant drop in contact angle was reported as a result of treatment. However, this plasma induced hydrophilic nature was not permanent. The contact angle increased with elapsed time after the treatment has stopped.

Callewaert et al. investigated the dynamic wetting behaviour of water and alkaline solution of KOH on polymer coated gold substrates [62]. The substrates were spin coated with PS_{159}-PAA_{62} and PS_{41}-PAA_{271} polymeric solutions and R_{rms} roughnesses of 2.4 nm and 0.6 nm were formed as a result of polymer coating respectively. A rise in advancing contact angle and a drop in receding contact angle is reported with decreasing roughness for both liquids. The contact angle hysteresis was

Table 3
Effect of roughness on contact angle/wettability

System and parameters	Roughness range	Observation	Reference
DI water/Cu	100–350 nm	Contact angle decreased linearly with increasing roughness (90° to 45°)	[33]
Water/pirosiloxiane	Plasma treatment on the surface/ micrographs indicate change in roughness	Ar plasma: 81° to 50° in 2 min O_2plasma: 81° to 14° in 5 min O_2/CF_4 plasma: 81° to 0° in 1 min	[60]
Water/Cu Water/Al	Variation of plasma irradiation time on surfaces subjected to polishing to different levels	Before irradiation: Cu: 89°–102°, Al: 54°–82°, Stainless steel: 61°–78° (mirror finish exhibited higher contact angles than other surfaces except for steel)	[61]
Water/stainless steel		Immediately after irradiation: Cu: 11°; Al: 3°; Cu: 6°	
Water, organic liquids/glass, wax and polymer surfaces	–	Increasing trend of contact angle with increasing roughness	[58]
Water/glass Isopropanol/glass Glycerin/glass	0.003 μm–3.6 μm	10°–78° (adv.); 6–16° (rec.) 0° 17°–62° (adv.); 12–13° (rec.)	[59]
Water/polymer coated gold	0.3 nm–2.7 nm	Adv.: 105° to 87° at pH 5.6 96° to 88° at pH 11 Rec.: 18° to 47° at pH 5.6 14° to 25° at pH 5.6	[62]
DI water/Cu DI water/stainless steel	–	Decreasing tendency of contact angle up to critical value of roughness	[38]
Silicone oils/glass	2 μm–50 μm	Additional regime in the spreading on rough surface	[57]
DI water, organic liquids/paraffin wax	Mechanically roughened to varying extents	Hysteresis decreased with decreasing roughness (from 61° to 4°) Paraffin wax/ethanol system did not show any dependency on roughness	[40]
Water/paraffin	Model surfaces (hemisphere and hemiround-rod)	Contact angles in the range 95°–125° are reported	[52]
Organic and polymeric liquids/glass	0.07 μm–40 μm	Dependence of empirical constants in the power law on roughness diminish as viscosity increases	[64]
Sn–Pb solder/Cu Pb-free solders/Cu	100–350 nm	Contact angle decreases with increasing roughness	[33]
Copper/MS Copper/SS	–	Decreasing contact angle with increasing roughness	[63]
Sn–Pb solder/copper	>50 μm	Extensive wetting	[42]

large on a surface with smaller roughness which is opposite to the trend observed by Volpe [58] and Kamusewitz [40].

Nicholas et al. analyzed the wetting behaviour of copper sessile drop on mild steel and stainless steel plates and reported the decreasing tendency of contact angle with increasing roughness [63]. Yost et al. investigated the wetting behaviour of Sn–Pb eutectic solders on very rough (>50 μm) copper surfaces (Ni substrates electroplated with copper) and concluded that for extensive wetting $\alpha > \theta$. They opined that rough/grooved surfaces provide an additional driving force for wetting as liquid solder flows into the valleys by capillary action [42]. Lin and Lin carried out number of experiments on wetting of DI water, Sn–Pb and Pb-free solders on surfaces of different roughnesses with R_a values varying from 98 nm to 297 nm [33]. They observed a general trend of decreasing contact angle with increasing surface roughness, as predicted by Wenzel. However, a large scatter was found in their experiments.

Table 3 summarizes the observations of various researchers on the effect of roughness on contact angle.

3.2. Heterogeneity of the surface

Surface cleanliness has an important influence on contact angle as any impurity present on the surface will make the surface heterogeneous [38]. Surface heterogeneity is inevitable due to various reasons. For example, polycrystallinity, impurities present on the surface, etc. make the surface heterogeneous. Fig. 17 is a schematic sketch of sessile drop placed on a composite surface. Heterogeneous surfaces cause metastable equilibrium state for the system resulting in multiple contact angles. Further, a contact line traversing on a heterogeneous surface will become pinned to the patches, which generally produces lower contact angles. The Cassie equation is generally used to explain a composite contact angle on a heterogeneous surface [15]:

$$\cos \theta_c = f_1 \cos \theta_1 + f_2 \cos \theta_2 \tag{11}$$

Here f_1 and f_2 represent the fractions of the surface occupied by the surface types 1 and 2 having contact angles θ_1 and θ_2 respectively. A little consideration will show that for a woven material like fabric cloth, the above formula reduces to:

$$\cos \theta_c = f_1 \cos \theta_1 - f_2 \tag{12}$$

since f_2 is the fraction of open air which makes $\cos \theta_2 = -1$, as $\theta = 180°$, for non-wetting situation. This is of practical significance for designing waterproofing fabrics.

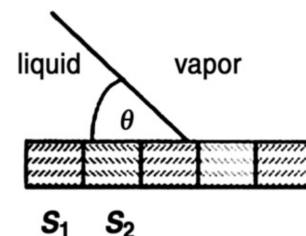

Fig. 17. Sessile drop placed on a composite surface [65].

Surface heterogeneity also results on a very rough surface due to the entrapment of air by the liquid [18]. The contact angle in such a composite surface may be given by:

$$\cos\theta_c = r f_1 \cos\theta_1 - f_2 \quad (13)$$

Fig. 18 shows a very rough surface with entrapped vapour phase beneath the spreading liquid giving rise to a composite situation.

3.3. Flux

The role of flux in wetting has far reaching consequences particularly in the spreading of metallic liquids. The reason is oxidation of surface of substrate as well as liquid. The breakdown of oxide film is vital to achieve true wetting in any system since the film present on the substrate surface or spreading liquid will alter the interfacial properties. To overcome the barrier effects of oxide films, fluxes are generally used [10]. The usage of flux in reactive wetting processes such as soldering has two major functions [3,4,66]:

- Chemical function — to provide a tarnish-free surface and to keep the surface clean by removing tarnish films from surfaces, breaking existing oxides and protecting the cleaned surfaces against re-oxidation.
- Physical function — to remove the reaction products from the surfaces to allow the solder to come into intimate contact with the base metal surfaces.

In soldering fluxes keep the solderable surfaces clean and tarnish-free and to influence the surface tension of solder in the direction of solder spreading by decreasing the contact angle [3,4,66,67]. The reactive surfaces present on the liquid solder and clean metal substrate are highly susceptible to contamination through adsorption, reaction and diffusion processes. The flux generally removes oxide layers from substrate and solder surface and improves wetting [10,68]. Fig. 19 shows the action of flux altering the wetting phenomenon.

Fluxes can be broadly classified into two categories, viz — inorganic and organic. The first category includes inorganic acids, salts and gases. These fluxes are not only fast acting but also corrosive in nature. Hence, cleaning is necessary after their use. Organic fluxes are comparatively milder than inorganic ones. They are either rosin base or resin base fluxes. These fluxes generally contain small quantity of activators so as to use successfully in general applications. No-clean fluxes have also been developed which do not require post-cleaning operations.

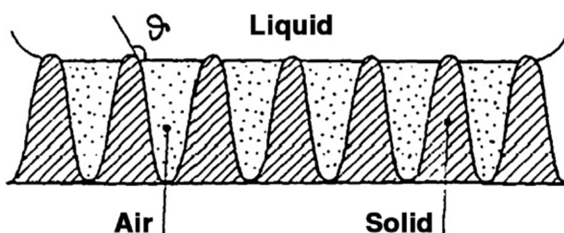

Fig. 18. Very rough surface with entrapped vapour phase beneath the spreading liquid [18].

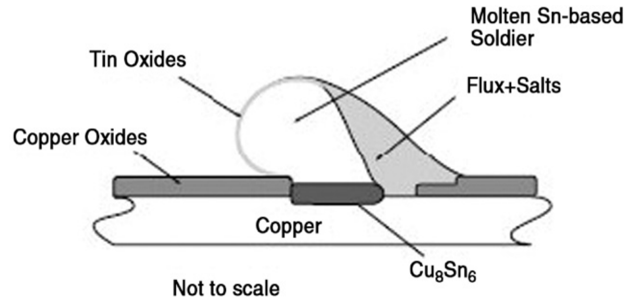

Fig. 19. Action of flux altering the wetting phenomenon [7].

Usage of rosin flux is a common industrial practice. Such a flux generally contains 40–60% rosin (by wt.%), 7–10% thickeners, 5–10% viscosity agents, about 2% activators and different solvents as a balance. Various constituents of flux should evaporate easily after fulfilling their function. Fig. 20 is a schematic representation of reflow soldering profile in which evaporation of various constituents of flux are indicated [66]. The rosin is typically dissolved in an organic vehicle combination of different alcohols to form the liquid solution. All the alcoholic solvents evaporate during pre-flow phase since they are light hydrocarbon compounds. Modifiers are heavier hydrocarbons and hence evaporate at the beginning of the heat-up in the reflow phase. Finally the rosin evaporates. It was found that the flux evaporation increases as the oxygen level in the atmosphere increases. Hence, the amount of residues will come down with increased purity of atmosphere.

However, the present tendency is to go for fluxless technology because number of industrial products cannot accommodate fluxes in the soldering process. For example, MEMS devices, sensors, biomedical devices, etc., need the component to be joined without using flux. Fluxless approaches fall into two basic categories. One is to use chemicals/plasma to remove the oxide layers where as the second is to produce solders in a non-oxidizing atmosphere and covering with a cap [7].

There is good agreement in the literature about that fluxes improve the wetting force by increasing the solid/vapour interfacial energy or by lowering the solid/liquid interfacial energy.

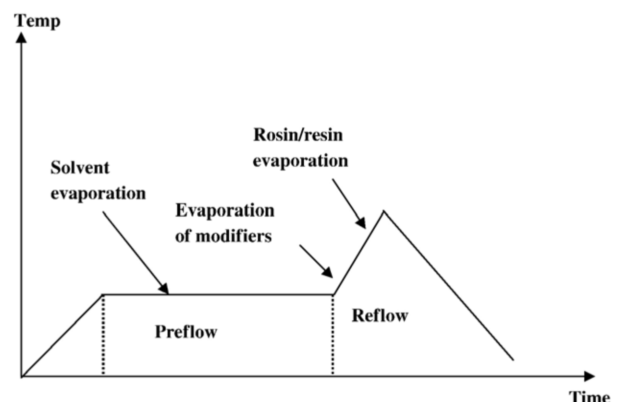

Fig. 20. Reflow soldering profile [66].

Takao et al. performed studies on action of flux on wettability for lead-based and lead-free solders [26]. Contact angles as well as interfacial tensions were measured in their investigations. Use of a halogen containing activated flux during wetting test of Sn–3.5Ag on Cu substrate resulted in a decrease of 5° in the contact angle and 0.064 N/m in the value of liquid solder/flux interfacial tension. Similarly the investigations of Lopez et al. on the flux assisted spreading of liquid aluminium on TiC substrate clearly showed that the replacement of solid/gas interface by solid/flux interface and liquid metal/gas interface by liquid metal/flux interface (of lower energies in both cases) enables spreading and wetting of liquid aluminum on TiC [10].

The experimental evaluation of the effect of low temperature fluxes on wetting by Plas et al. revealed that the rate of wetting increased as the acid content in the flux increased and as the temperature of the solder bath is increased [41]. The rate of wetting is dependent on the degree of oxide removal, which is a function of oxide concentration as well as the temperature. The effect of flux on wettability of various reactive spreading systems is summarized in Table 4.

3.4. Temperature

The wetting behaviour of liquid on solid is sensitive to temperature changes as temperature affects the number of properties of liquid as well as substrate. Viscosity, surface tension, oxidation behaviour, reaction rate, etc. are few such properties. It is a common observation that there is a decrease in viscosity and surface tension of the liquid with increase in temperature. Hence, wettability should improve in any systems with increase in temperatures [12]. Even in reactive wetting systems the diffusion rate generally increases with increase in temperature. However, exceptions may exist which can be attributed to opposite effects due to phase changes, reactivity changes, oxidation, etc. This type of trend is often observed during the evaluation of solders in the presence of flux at various temperatures. Apart from the general effects of temperature on the properties of spreading liquid like viscosity, surface tension, etc. there will be two important points to be taken into account. The increase in temperature results in severe oxidation in most of the metals. Solders are no exception. The oxide layers present on the surface of the spreading liquid as well as on the substrate surface alter the interfacial properties and cause inferior wetting. The function of flux is to overcome this trouble by removing the oxides and other contaminants from the surface so that intimate contact between solder and substrate as already discussed earlier. These fluxes composed of organic solvents or halides and are generally active at temperatures about 10–20° below the melting/liquidus temperatures of solders. The increase in the temperature beyond their activation temperature may cause evaporation of the flux. As a result there may be no availability of flux for removing oxides. This might be the reason for poorer wettability reported by some researchers at higher temperatures.

The observations of Kandlikar et al. on boiling phenomenon of DI water on copper and stainless steel surface indicated that both advancing and receding dynamic contact angle become equal at the temperature corresponding to critical heat flux at which transition of boiling phenomenon takes place [38].

Coninck et al investigated the effect of temperature on contact angle relaxation during spreading of squalane on PET and on the liquid properties [72]. They reported a moderate drop in surface tension and a substantial drop in viscosity of squalane in the temperature range of 10–55 °C. Further, a variation of −0.15°/°C increase was observed in their experiments.

Bukat et al. carried out investigations on the effect of temperature on wettability of lead-free solders and reported a decrease in interfacial tension and an increase in wetting force

Table 4
Effect of flux on contact angle/wettability

System	Variable	Observation	Reference
Pb–Sn/Cu Bi–In–Pb–Sn/Cu	Acid content of the flux	Rate of wetting increases as the acid content in the flux increases	[41]
Sn–Pb/Cu Sn–Ag/Cu Sn–Ag–Cu/Cu Sn–Zn/Cu	Flux type (NC, RMA and WS) [a]	For Sn–Pb solders use of WS flux resulted in best wetting (31, 22 and 12°) where as for Sn–Ag solder NC found better (39, 41,63°) Sn–Ag and SAC alloys can be soldered with RMC fluxes where as Sn–Zn solders can only be soldered with RA flux	[69]
Lead–tin and lead-free solders Ceramic substrates plated with Ni/Au	Type of flux (WS, NC etc.) [a]	Environmental friendly water soluble fluxes can be used without degrading wetting	[70]
Sn–Pb and SAC solders Cu and Cu/Ni/Au pads	Type of flux (WS, NC, RA, RMA) [a]	No significant difference in the relaxation behaviour as well as terminal contact angle	[30]
Sn–Pb, Sn–Ag, Sn–Bi, Sn–Zn/Cu	Type of flux (aqueous clean and no clean)	Pb-free alloys showed lower wetting forces than Sn–Pb solder while using either type of flux Higher wetting forces are reported when aqueous clean flux is employed Sn–Zn solder did not show any wetting when no-clean flux is used Use of more active flux is needed to achieve same degree of wetting with Pb-free alloys as obtained with Sn–Pb alloys	[71]
Sn/Cu Sn–Zn solder/Cu	Concentration of metallo-organic compound in the flux	CA for Sn/Cu is 37° and that for Sn–Zn/Cu is 89° (both with RMA flux) The lowest values (25–30°) are obtained with Sn–Zn solder when 15% metallo-organic compound is present in the flux	[67]
Molten Al/TiC	With/without flux	Use of flux reduces the effect of atmosphere on spreading Wetting becomes more sensitive to temperature in the presence of flux	[10]

[a] NC: no clean; WS: water soluble; RA: Rosin activated; RMA: Rosin mildly activated.

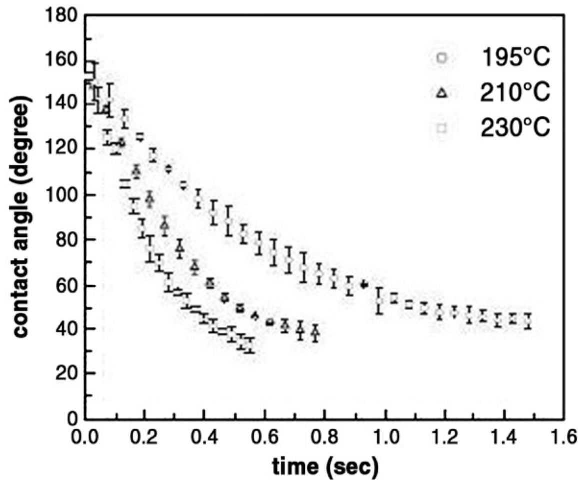

Fig. 21. Effect of temperature on contact angle relaxation [30].

with increase in solder bath temperature. Both of these factors contribute to the improvement in wettability [25]. Martorano et al. also made similar observations while investigating the effect of solder bath temperature on wetting balance curve of tin–zinc–silver solder alloy [44]. Decreasing the temperature of the solder bath resulted in the significant decrease in wetting rate. Possible reasons for this decrease are decrease in liquid viscosity and reduction in efficacy of flux with increase in solder bath temperature. Further, partial solidification of solder bath at lower temperatures contributes to the reduction in wetting rate. On the other hand, an increase in bath temperature increases rapidity of wetting kinetics.

Kang et al. carried out experimental investigations to study the dependence of contact angle and wetting on temperature by eutectic tin–lead and lead-free Sn–4Ag–0.5Cu alloys [30]. They observed that an increase in temperature resulted in speeding up of wetting process. As the temperature increases, the reactivity between the solder and the substrate material also increases due to the temperature dependence of diffusion process. Further, the viscosity of the molten solder, like any other liquids, decreases with increase in temperature and hence, results in decrease of surface tension. All these factors contribute to higher rate of spreading at elevated temperatures as seen from the Fig. 21. A decrease in duration time (the time required for the decrease in contact angle from 140° to 50°) of about 70% was observed in their experiments for the temperature change from 190 °C to 230 °C (See Fig. 22).

Investigations of Wu et al. on wetting of Sn–9Zn–*x*RE solders on Cu substrates indicated a drop in contact angle of 9–14° when the temperature was increased from 245° to 290° [69]. Saiz et al. studied the spreading of Sn–Ag–Bi solders on Fe–Ni alloys at 250 °C and 450 °C and recorded contact angles 70–85° and 50–65° respectively [31]. This clearly indicates that the temperature is responsible for reduction in contact angle.

Kang and Baldwin investigated the effect of temperature on dynamics of wetting during spreading of eutectic tin–lead solder [73]. But the temperature range selected in their experiment was too small (193 °C and 203 °C) to show any effect on wetting dynamics.

Studies of Lopez and Kennedy indicated that the wetting process is thermally activated since the process clearly showed temperature dependency [10]. The spreading time showed Arrhenius type of behaviour:

$$\frac{1}{t_o} = K\exp\left[-\frac{E_a}{RT}\right] \tag{14}$$

where t_o is the spreading time.

The activation energy was calculated by plotting $\ln(1/t_o)$ versus $1/T$ and finding the slope of the graph obtained as pointed out in Fig. 23.

Shen et al. attempted to assess the effect of temperature on the spreading kinetics in a reactive wetting system [74]. The decreasing rate and magnitude of contact angle in Al/SiO_2 system were strongly dependent on the temperature. In general, the higher the temperature, the faster the relaxation and the smaller the final contact angle. However, some anomalies were observed in this behaviour and were primarily because of phase changes taking place in the reaction product (Al_2O_3).

The results of the investigations on the effect of temperature on spreading are summarized in Table 5.

3.5. Trace elements

Alloying additions to binary and ternary lead-free solders are generally made in order to improve wetting and mechanical properties. In fact, it is a method to improve the wetting of a

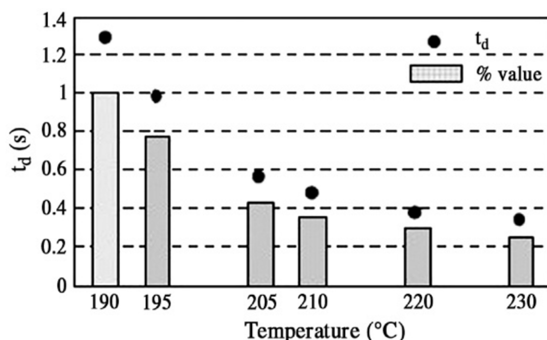

Fig. 22. Effect of temperature on duration time [30].

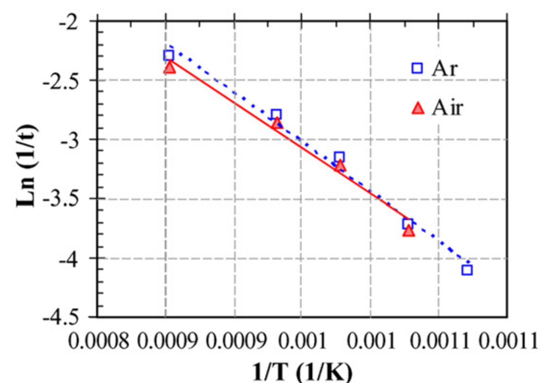

Fig. 23. Determination of activation energy for spreading [10].

Table 5
Effect of temperature on contact angle/wettability

Liquid	Substrate	Temperature	Observation	Reference
Sn–Pb and few Pb-free solders	Cu	–	Increase in temperature increases the wettability	[9]
Sn–Pb and few Pb-free solders	PTFE, Cu	–	Drop in IFT of solder Rise in wetting force Drop in wetting time	[25]
Sn–Pb and Bi–In–Pb–Sn	Cu	–	Increase in rate of wetting Max. wetting force is obtained at 160 °C	[41]
Sn	Cu	240, 250, 260 and 280 °C	Effect of substrate thickness on spreading kinetics fades away as the bath temperature is increased	[44]
Sn–Pb and SAC solders	Cu/Ni/Au and Cu pads	190–230 °C	Wetting rate increased with increase in temperature	[30]
Sn–Pb–Bi solders	Cu	160–255 °C	Solderability of Bi solders are better than Sn–Pb solders at lower temperatures	[75]
Sn–Pb and Pb-free solders	Cu	230–250 °C	At 230 °C, SZ–Al solder showed better wettability than SAC solder	[76]
Sn–Ag–Bi	Fe–Ni alloys	250°C 450°C	Significant drop in contact angle (70–85° at 250 °C and 50–65° at 450 °C)	[31]
Sn	Cu	–	Slight increase in substrate temperature results in large increase in spreading rate Spreading mechanism changes at 327–330 °C from thermally activated process to thermally non-activated process Spreading rate shows 1/3 order dependency on time up to 327 °C and 1/5 order thereafter	[68]
Sn	Au	250–430 °C	Limited spreading at low temperatures, rapid spreading at intermediate temperature and extensive spreading at higher temperatures are observed Perfect wetting behaviour at 430 °C	[77]
Sn–Pb	Au plated Cu	193 °C 203 °C	No effect of temperature (12°)	[73]

given substrate by a given metal not only in soldering but also in brazing. The spreading metal is alloyed with a chemical species which reacts with the substrate to form a dense layer of solid reaction product. This reaction product is better wetted by the metal than the original substrate [78].

Chen et al. investigated the influence of gallium addition on wettability of Sn–Zn–Ag and Sn–Zn–Ag–Al lead-free solder alloys [79]. The selection of Sn–Zn alloys were made since the melting point/liquidus of Sn–Zn alloys is very close to traditional Sn–Pb eutectic solders. It has been shown in their experiments that the increase in gallium addition resulted in significant reduction in wetting time and increase in wetting force. Wetting time reduced from 2.5 s at 0% Ga to 0.5 s at 3% Ga in the alloy. However, Ga is reported to decrease the microhardness and increase the pasty range at concentrations >2%.

Investigations on rare earth addition to lead-free solders indicated that Ce and La additions improved wetting in most of the lead-free alloys [29,69,80]. For example, contact angle of Sn–Ag eutectic alloy reduced from 47° to 41° on addition of 0.25% RE. Similar results were found during the RE addition to Sn–Ag–Cu and Sn–Zn alloys. However, higher RE addition deteriorated wetting behaviour by lowering the wetting force and by increasing contact angle. The addition of RE is found to reduce the surface tension between the solder and the flux since it accumulates at the solder/ flux interface, thereby, reduces the contact angle [69]. But, at higher amounts they increase the viscosity of the molten solder, tend to oxidize easily and hence adversely affect the wetting. Fig. 24 shows the effect of RE addition on contact angle and wetting force of Sn–Ag solders.

Wnag et al. investigated the effect of Zn addition to lead-free Sn–0.7Cu solder alloy on wetting behaviour of the alloy with Cu substrate [34]. The Zn is varied in the range 0–1 wt. % in the alloy during wetting balance experiments. A deterioration of wetting is observed in their experiments as contact angle increased from 42° for zero zinc addition to 50° at 1% Zn addition to the alloy. But the addition of copper to Sn–9Zn solder alloy was found to be very much beneficial [32]. It was reported that 10% addition of copper would bring down the contact angle of solder on Cu substrate from non-wetting situation of 120±8° to 54±6° (see Fig. 25) in which 0.25% to 1% addition brought a greatest drop in the contact angle. It was also reported that addition of Bi [81] or Al [76] improved the wettability of Sn–Zn solders. The addition of Bi to the conventional Sn–60Pb is found to decrease the surface tension of solder alloy as well as to help in preventing the dewetting by lowering the surface concentration of Pb atoms [82].

Table 6 is the collection of results related to effect of trace impurity/alloying addition on wettability and contact angle.

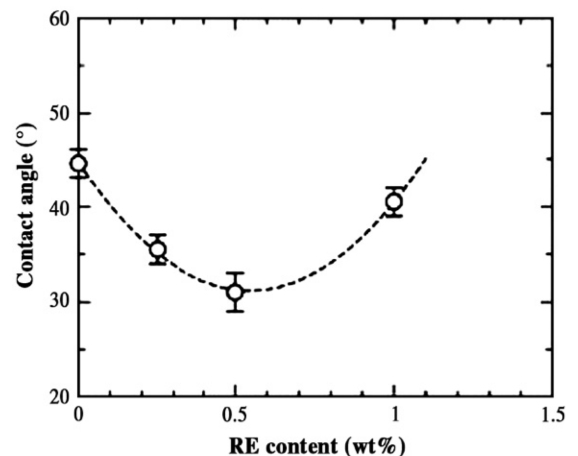

Fig. 24. Effect of RE addition on contact angle of Sn–Ag solders [80].

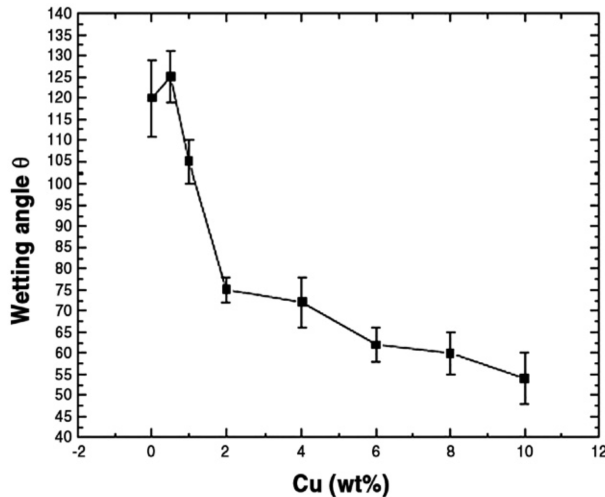

Fig. 25. Effect of copper addition on contact angle of Sn–Zn solders [32].

3.6. Atmosphere

The atmosphere plays a prominent role in spreading of metallic liquids like solders. It has been established that the reduction in residual oxygen level (ROL) in the atmosphere causes the spreading to start at lower temperatures. The oxide surface on the substrate is known to deteriorate wetting and hence use of flux and/or inert atmosphere is inevitable to achieve good wetting [28,66,89]. Nitrogen is generally used to displace oxygen since it is inert and chemically non-reactive with most of the metals. The soldering process is benefited by this inertness of nitrogen because solderable metal surfaces can be protected from oxidation during heat-up and proper flux action can thus be ensured. Improved wetting is observed in most of the spreading trials when carried out in N_2 atmosphere than in air particularly in soldering [45]. Good wetting or solderability is generally attributed to low surface tension of the spreading liquid. However, the surface tensions of oxides are significantly lower than those of the corresponding metals. Therefore, an oxidized liquid solder is expected to exhibit better wetting than the unoxidized solder, which is contrary to the observed results. The main reason for this is that the wetting is a complex phenomenon that depends not only on liquid surface tension but also on surface properties of the substrate. The atmosphere that caused oxidation of liquid solder would definitely cause oxidation of the substrate also. Further the process will add contaminants to the surface. The net effect is deterioration of wetting.

The presence of inert atmosphere is also helpful in improving the efficiency/functioning of fluxes in reactive spreading processes [66]. For example, in soldering under normal atmospheric conditions and at ordinary oxygen levels, oxygen can diffuse into the flux components and attach to the bonds in the organic matter. As a result polarity as well as secondary bond forces of the flux constituents well increase, which in turn causes the increased resistance to break-up or evaporation. The net result is a decrease in the efficiency of flux, an increase in the amount of flux residues and reduced evaporation of flux components. On the other hand, the use of inert atmosphere like nitrogen will decrease the oxygen level in the atmosphere thereby increasing its purity. Consequently, amount of residue will come down; evaporation of flux will be complete and wetting will be enhanced. Fig. 26 shows how area of spread of solder paste decreases as the oxygen level in the atmosphere increases.

3.7. Liquid properties

Viscosity, surface tension and density are the three important properties that affect spreading of a liquid drop over a solid substrate. The study of each of these factors on wetting independently is difficult as the evolution of contact angle is governed by these forces which exist at various stages of spreading simultaneously.

Table 6
Effect of trace impurity addition on contact angle/wettability

System	Trace element added	Observation	Reference
SAC/Cu	RE (Ce, La)	RE addition resulted in improvement of wettability Higher addition resulted in degradation	[29,69,80]
SAC/Cu, Cu/Ni	Sb, Bi	Increase in Sb content decreased the rate of wetting	[83]
Sn/Cu	Ag, Bi, Zn, In	Ag and In did not bring any improvement in wetting Bi improved wetting and Zn deteriorated wetting	[84]
SAC/OSP coated substrates with various PCB finish	Bi, Pb	Pb addition did not bring any change in the wetting temperature Increasing Bi decreased wetting temperature	[85]
Sn–Zn–Ag–Al/Cu	Ga (0.5–3%)	Wetting time decreased and wetting force increased with Ga content	[79]
Sn–Zn/Cu	Ag (0.5–3.5%)	Maximum adhesion strength is obtained at 1.5% of Ag	[86]
SAC/Cu	Sb (0–2%)	IMC layer became thin and grains refined with increasing Sb addition	[87]
SAC/Cu and Cu–Ni–Au	Ni, Ge	Improvement in interfacial reaction	[88]
Sn–Zn	Al	Wettability improved significantly Best results obtained at 60 ppm addition	[76]
Sn–Ag	Bi	Bi content did not affect either surface energy or spreading rate	[31]
Sn–Zn	Cu (0–10%)	Wettability improved (120° to 54°) Significant improvement at 0–2% addition	[32]
Sn–Bi–In/Cu	Bi and In	Bi decreased wetting angle and In increased wetting angle	[21]
Sn–Pb	Pb, Bi	Pb addition to Sn–Pb alloy decreased ST and to Bi–Pb alloy increased ST	[80]
Sn–Bi		Bi addition to Sn–Bi alloy decreased ST	
Bi–Pb		Bi prevented de-wetting	

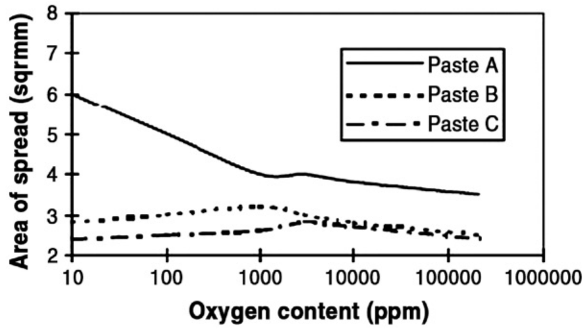

Fig. 26. Effect of atmosphere on area of spread of solder paste [66].

As deduced from the classic Young's equation, a lower contact angle or better wetting is expected whenever the liquid/vapour interfacial tension is low. In other words, wettability of a surface for a liquid can be improved by reducing the liquid surface tension. Surfactants are generally used with this intension. Similarly the use of flux in soldering is justified with improved wetting. Sikalo et al. reported that a small drop of liquid of small surface tension splashes more while impacting on a smooth plate than a drop of high surface tension does [59].

It is well known that any spreading activity will be resisted by the viscosity of the spreading liquid. Hence, it is reasonable to expect that a droplet of higher viscosity liquid spreads little compared to that of lower viscosity and it is found true in a number of studies. This is because, higher viscous dissipation reduces the rate of spread. Further, it is reported that a spreading viscous drop approaches its maximum spread or equilibrium in a shorter period of time. Sikalo et al. observed that the maximum spread of highly viscous glycerin droplet is much less than that for water droplet [59]. It is also reported that low viscous and smaller drops spread faster [90].

The effect of gravity is generally not taken into account in wetting studies since the liquid drops involved in the experiments are small enough to affect the drop shape. It is accepted that if the drop radius is less than the capillary length (the square root of the ratio of liquid surface tension to the mass of the liquid drop) the gravity force does not affect the spreading process. Number of investigations attempted to quantify the effect of gravity and found it as negligibly small [37,59,90].

4. Thermodynamics of wetting

4.1. Inert systems

The formation or establishment of interface during wetting of a solid by a liquid is ruled by thermodynamic principle of energy reduction. The elimination of two surfaces to form an interface reduces the total energy of system. Hence, the thermodynamic condition for wetting to occur can be written as [11]:

$$\gamma_{sv} > \gamma_{sl} > \gamma_{lv} \tag{15}$$

Further, using the definition of spreading coefficient S (which is equal to $\gamma_{sv} - (\gamma_{sl} + \gamma_{lv})$), it can be stated that when $S > 0$, it is energetically possible for a liquid to spread over a solid surface.

For an ideal (smooth, homogeneous, rigid and insoluble) solid surface, the thermodynamic equilibrium condition is given by Young's equation [35,36] and the same can be derived by using the energy minimization concept as well [15].

It is observed that a liquid placed on solid remains as a drop having a definite angle of contact between the liquid and solid phases (see Fig. 3).

The change in surface free energy (ΔG^s) accompanying a small displacement of liquid such that the change in area of solid covered (ΔA) is

$$\Delta G^s = \Delta A(\gamma_{sl} - \gamma_{sv}) + \Delta A \gamma_{lv} \cos(\theta - \Delta\theta) \tag{16}$$

At equilibrium

$$\lim_{\Delta A \to 0} \frac{\Delta G^s}{\Delta A} = 0 \tag{17}$$

and therefore,

$$\gamma_{sl} - \gamma_{sv} + \gamma_{lv} \cos\theta = 0 \tag{18}$$

The above equilibrium condition presumes uniformity of temperatures and chemical potentials.

An extensive thermodynamic treatment of contact angle equilibrium on real surfaces is given by Marmur [35,36]. Considering a specific system of drop of non-volatile liquid on a rigid and insoluble solid, the mechanical equilibrium condition can be written assuming a two dimensional axisymmetric drop and neglecting the effect of external field as follows:

$$\mathrm{d}\int_0^X \left[\gamma_{lv}\sqrt{1 + (y')^2} + (\gamma_{sl} - \gamma_{sv}) r(x)\right] x^k \mathrm{d}x = 0 \tag{19}$$

Here r is the local ratio between the true surface area of the solid under the liquid drop and corresponding nominal area. The above equation may be interpreted as the condition for minimum free energy of the two interfaces (the first term corresponds to liquid–vapour interface and the second one represents the free energy of the solid–liquid and solid–vapour interfaces).

General equation for apparent contact angle can be derived by solving the above equation under the constraint of constant volume and suitable boundary conditions:

$$\cos\theta = \frac{r(x)(\gamma_{sv} - \gamma_{sl})}{\gamma_{lf}(1 - y'_s \tan\theta)} \tag{20}$$

In the simplest case of ideal (smooth, homogeneous, rigid and insoluble) solid and constant interfacial tensions, the above equation reduces to Young's equation:

$$\cos\theta_y = \frac{\gamma_{sv} - \gamma_{sl}}{\gamma_{lf}} \tag{21}$$

For a chemically homogeneous but rough surface, $r(x)$ can be expressed as:

$$r(x) = |\cos\alpha|^{-1} \tag{22}$$

where α is the angle which the solid surface makes with the x-axis. Using this, the expression for apparent contact angle can be written as:

$$\cos\,\theta = \frac{\cos\,\theta_y}{|\cos\,\alpha(x)|(1-\tan\,\alpha(x)\tan\,\theta)} \tag{23}$$

$$\text{or } \theta = \theta_y - \alpha(x) \qquad \text{for } \alpha < \pi/2 \tag{24}$$

$$\text{and } \theta = \theta_y + \pi - \alpha(x) \qquad \text{for } \alpha > \pi/2 \tag{25}$$

On the other hand, for smooth but chemically heterogeneous solid surfaces, $r(x)=1$, the apparent contact angle is:

$$\cos\,\theta = \cos\,\theta_y(x) \tag{26}$$

Thus, from the thermodynamic point of view, the above discussion is summarized as given below:

- For an ideal solid, the apparent and intrinsic contact angles are identical and the Young's equation predicts a single value for the equilibrium contact angle.
- The apparent contact angle on a homogeneous rough surface is simply the difference between the intrinsic contact angle and the local angle of inclination of the solid surface.
- For smooth but chemically heterogeneous solid surfaces, the apparent contact angle always equals to the local intrinsic angle at the contact line.
- The thermodynamic equation for contact angle indicates that multiple contact angles are possible on rough or heterogeneous surfaces.

4.2. Reactive systems

In reactive systems, wetting frequently occurs with extensive chemical reaction and the formation of a new solid compound at spreading liquid/reactive substrate interface. For example, during soldering on a copper substrate the process will always result in the formation of intermetallics of Sn and Cu. Similarly, in the reactive metal penetration technique of producing the novel composites, a molten metal wets, penetrates and reacts with either a dense or a porous ceramic preform, converting it to a metal-ceramic composite [74]. Hence, the nature and rate of spreading is influenced by the reaction between spreading liquid and reactive substrate material. The quality of bonding between the constituents is determined by wettability as well as reactivity [91]. The reactive wetting is advantageous in number of cases since even a small addition of a constituent to a spreading liquid reacts with the substrate material and causes pronounced improvement in wetting. This phenomenon is exploited in brazing and soldering [92].

However, concept of thermodynamics of wetting already discussed is limited only to inert systems. Because, in reactive wetting, the wetting is followed by material transport at the solid/liquid interface. A chemical reaction generally occurs between the mating surfaces and the resultant chemical bonds are responsible for wetting. Hence, according to conventional thermodynamic approach, the wetting should be possible whenever ΔG_r for the interfacial reaction is negative [93]. Contact angle is an accepted measure of wettability at the interface. The familiar Young's equation suggests that a system is considered to be wetting when the wettability parameter γ_{LV} $\cos\theta > 0$ [because $\gamma_{LV}\cos\theta = \gamma_{SV} - \gamma_{SL}$)]. Hence, a plot of γ_{LV} $\cos\theta$ versus ΔG_r could be used to predict wetting. A sample plot is shown in Fig. 27 which can be divided into four regions. I quadrant represents the wetting regime where as IV quadrant corresponds to non-wetting regime. On the other hand the quadrants II and II have no physical meanings.

Chidambaram et al. pointed out an important disadvantage of this approach [93]. The wettability of Mn, Cr and Cu–Ti alloys with α-alumina lies in the physically meaningless regimes. However, experiments indicate that the wetting occurs in these systems.

The above approach is based on bulk thermodynamics and disagreement between the theoretical predictions and experimental observations cannot be explained by bulk thermodynamics. The surface of a material can be treated as a separate phase in equilibrium with the bulk. Further, $\Delta G_{surface}$ would be less negative than ΔG_{bulk} since the atoms on the surface are missing half their nearest neighbours and are loosely bound compared to the atoms in the bulk. As a result, reduction of the surface phase requires less energy than that of the bulk phase. Therefore, Gibbs free energy of wetting, ΔG_w (the free energy change for the surface reaction) should be much less than ΔG_r. This suggests that wetting is still possible in systems where bulk reaction between the phases may not be thermodynamically feasible.

Hence, the wettability map using ΔG_w and γ_{LV} $\cos\theta$ could give a better picture about wettability in various systems (particularly in metal-ceramic systems). Six regions can be identified in such a map (Fig. 28). Regions III, IV and V are physically meaningless regimes whereas region VI is non-wetting regime. Region I is the wetting regime and region II is a region which predicts wetting due to surface wetting. In this region, ΔG_w is negative and ΔG_r is positive. Cr, Ti, Mn and Cu–Ti alloys fall in the region II where wetting is possible but no bulk reaction can occur [93].

Contreras et al. investigated spreading of Al and Mg on TiC substrates in the temperature range of 800–1000 °C [91]. It was observed that aluminium wets TiC at all temperatures studied whereas Mg was able to wet the surface only at and above 900 °C. The degree of wetting is the result of the establishment of chemical equilibrium bonds achieved by the mutual saturation of the free valences of the contacting species. When the molten aluminium is in real contact with the surface of TiC, the spreading is found to be driven solely by chemical reaction occurring at the interface. The strength of binding between the phases can be assessed by determining the work of adhesion, W_a, defined as follows:

$$W_a = \gamma_{lv}(1+\cos\,\theta) \tag{27}$$

Hence, the condition for perfect wetting in a reactive system is $W_a \geq \gamma_{lv}$, since the contact angle in the above situation is 0°.

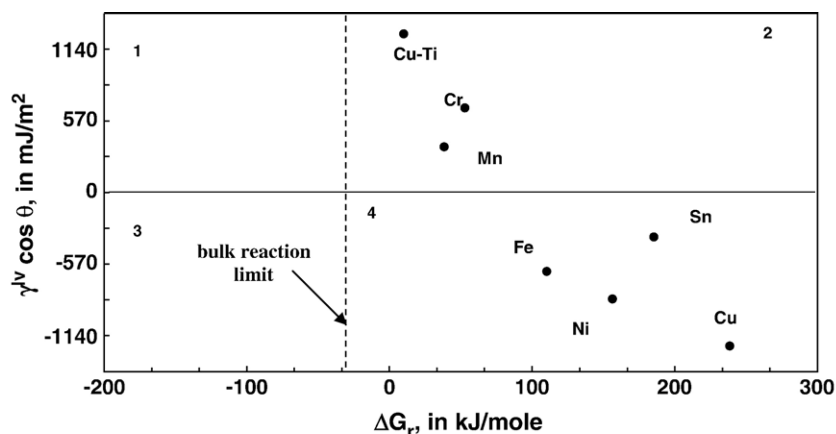

Fig. 27. Thermodynamic wettability map for the bulk material [93].

Eustathopoulos and co-workers [17,78,94–98] carried out extensive work in the field of reactive wetting. They studied wetting behaviour by sessile drop technique in number of reactive systems that includes the systems with good wetting as well as non-wetting behaviour in order to analyze the mechanism of wetting and to model the complex contact angle relaxation. Initially it was thought that the interfacial energy change affected by the interfacial reaction could be a major cause for enhanced wetting in reactive systems [98] and hence following equation was proposed for smallest contact angle in a reactive system with limited/moderate reactivity:

$$\cos\theta_{\min} = \cos\theta_{o} - \frac{\Delta\gamma_{r}}{\gamma_{LV}} - \frac{\Delta G_{r}}{\gamma_{LV}} \tag{28}$$

where γ_{LV} is the surface tension of the liquid, θ_o is contact angle on the substrate in the absence of any reaction, $\Delta\gamma_r$ represent the change in interfacial energy due to interfacial reaction and ΔG_r is the change in free energy per unit area released by the reaction of the material contained in the immediate vicinity of the metal/substrate interface. However, it was found from the later experiments [94,96] that the main effect of interfacial reaction on wetting is a change in the relevant energies of the system and not linked to the free energy change produced by the reaction. Further, it was observed that the steady state contact angle is almost the same as the contact angle obtained on the reaction product itself [17]. For example, steady state contact angle in the reactive CuSi/C_v system is nearly equal to the contact angle of the alloy on SiC. The observation is similar for the wetting of Cu–Cr alloy on C_v substarte.

On the basis of this observation, Eustathopoulos [99] proposed reaction product control (RPC) model to explain the reactive wetting behaviour (Fig. 29). According to this model, the final degree of wetting and the spreading kinetics are controlled by the new compound formed at the interface and not by the parent base metal. The initial contact angle obtained in a reactive system is the contact angle on the unreacted substrate where as after a transient stage, a quasi-steady configuration is established at the triple line where the advance of the liquid is hindered by the presence of a non-wettable substrate in front of the triple line. Hence, the only way to move ahead is by lateral growth of wettable reaction product layer until the dynamic contact angle becomes equal to the equilibrium contact angle for the liquid on the reaction product.

5. Kinetics of wetting

Thermodynamics or simple energetics is insufficient for considering the kinetic behaviour of fluids. Problems involving

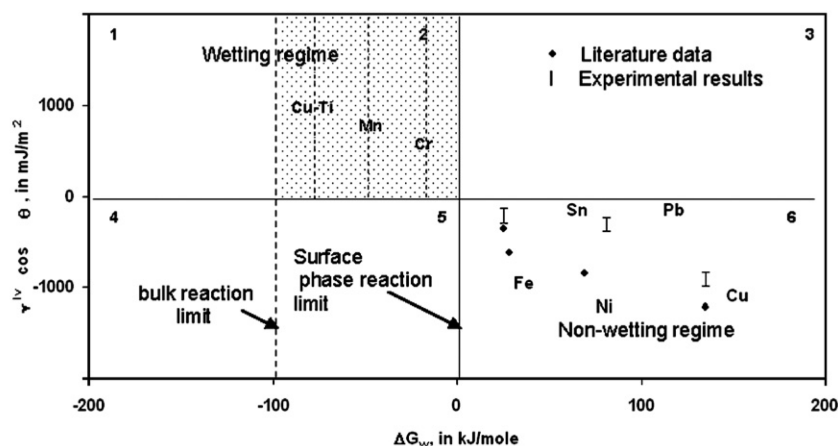

Fig. 28. Thermodynamic wettability map for the surface material [93].

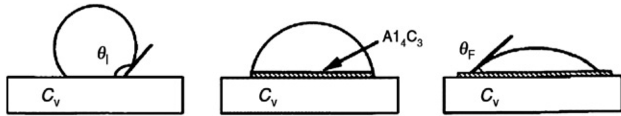

Fig. 29. RPC model for reactive wetting (stages of reactive wetting of liquid aluminium on vitreous carbon substrate) [17,95,99].

fluid flow rates, dynamic contact angles, contact angle hysteresis, shape and stability of liquid–fluid interfaces during flow are generally not amenable to solution by energy consideration alone. In such cases, a consideration of the forces acting in the system, i.e., the dynamics rather than the thermodynamics or energetics is more helpful [100]. Apart from the fundamental problem whether a given solid is wetted by the liquid in question, many of the practical applications require the precise knowledge of the rates of the wetting processes [101]. Consider the spreading of liquid drop on a flat solid substrate. When such a liquid is placed on the substrate, capillary forces drive the interface spontaneously towards equilibrium. As the drop spreads, the contact angle θ relaxes from its initial maximum value of 180° (at the moment of contact) to its equilibrium value (in case of partial wetting) or to 0° (in case of complete wetting. Although wetting has been studied since long, many fundamental problems are still open, particularly those related to the kinetics of contact line movement. Generally it is presented by using time/velocity dependence of dynamic contact angle. The dynamic contact angle has been correlated with the velocity of the contact line in molecular kinetic, hydrodynamic and combined approaches as well as in many empirical approaches [1].

Number of researchers studied the kinetics of spreading by utilizing forced spreading (i.e. droplet impact on a flat substrate) or self (spontaneous) spreading (i.e., placing a sessile drop on a flat substrate) and then recording the motion of the drop [2,38,77,102–110]. The images are processed for the determination of dynamic wetting properties. Laboratory studies of droplet impact have been done using molten metal or hydrocarbon droplets (diameters ranging from 2 mm to 4 mm and impact velocities in the range 1–3 m/s). However, practical applications encompass a very large range of droplet sizes (10 µm to 1 mm), materials (waxes, polymers, metals, ceramics, etc.) and impact velocities (1 m/s to 1000 m/s). Hence, it is customary to express the experimental results using dimensionless parameters. Following is a list of common dimensionless parameters employed in the wetting studies [1,30,64,68,90]:

- Dimensionless radius
- Normalized area
- Spread factor
- Reynolds number
- Bond number
- Weber number
- Capillary number

These dimensionless parameters are briefly discussed here.

Dimensionless radius: Dimensionless radius of drop is used as spread parameter in number of investigations. It is defined as

$$\frac{R}{R_o} \tag{29}$$

where R is the measured radius of the spreading drop and R_o is the radius of the drop when contact angle, $\theta = 90°$. With spherical cap approximation and assuming constant volume, R_o can be found as:

$$R_o = \left[\frac{3m}{2\pi\rho}\right]^{1/3} \tag{30}$$

Here m and ρ represent mass and density of the liquid respectively.

Normalized area: Number of researchers used instantaneous drop base area normalized with $V^{2/3}$, where V is the drop volume, in spreading studies. Here the assumption is that there is no loss of liquid due to evaporation or adsorption so that volume of the drop is constant.

Spread factor $\left(\frac{D}{D_o}\right)$: Normalizing dynamic drop base diameter (D) with initial value of sphere diameter (D_o) at the starting point yields spread factor which is used as a measure of spreading in number of studies.

Reynolds number (Re): A very important dimensionless number used extensively in all fields involving fluid flow. It can be expressed as a ratio of inertia forces to viscous forces. This number is generally used as a demarcation value for the flow patterns whether it is laminar or turbulent.

$$R_e = \frac{\rho U D}{\mu} \tag{31}$$

Bond number (Bo): An estimate of relative importance of gravity with capillary forces can be made with the help of Bond number. It can be expressed as a ratio of gravity forces to surface tension forces.

$$Bo = \frac{g(\rho_l - \rho_v)l^2}{\gamma} \tag{32}$$

When $Bo < 1$, capillary forces are expected to dominate gravity during spreading and flow can be studied by making spherical cap approximation for the drop profile.

Weber number (We): The relative importance of inertia with respect to capillary forces can be determined by using Weber number, which is defined as follows.

$$We = \frac{\rho U^2 D}{\gamma} \tag{33}$$

A low value of We indicates that there is no contribution from inertia to spreading.

Capillary number (Ca): It is generally regarded as dimensionless contact line speed and is treated as the ratio of viscous forces to surface tension forces. It can also be expressed as a

ratio of *We* to *Re*. It is commonly used in the evaluation of wettability of droplets impacting onto a substrate in order to determine dominating force among inertia and capillary.

$$Ca = \frac{\mu U}{\gamma} \tag{34}$$

In spreading models, it is quite common to express kinetics in terms of dynamic contact angle or base radius as a function of *Ca* [77].

While investigating the drop spreading kinetics, if the surface tension of the liquid/air interface is dominant force over gravity and viscous dissipation, the shape can be approximated as truncated sphere. A small value for both *Bo* and *Ca* are needed to justify this assumption [30].

5.1. Inert systems

If the liquid is capable of wetting the bare substrate without reaction, wetting kinetics can be determined by liquid surface tension and viscosity [92]. Most of the data on spreading of non-metallic drops on inert solids can be empirically correlated by the power law equation: $A = kt^n$ or $A' = k\tau^n$, where A is the measured liquid–solid contact area, A' is the dimensionless drop base area (normalized with respect to $(V)^{2/3}$, t is the time, τ is the dimensionless time (equal to $\sigma t/(\mu V^{1/3})$, k and n are empirical constants, V is drop volume, σ is the liquid surface tension and μ is the liquid viscosity [1,98]. The time dependence of dimensionless drop base area is empirically confirmed by number of researchers and obtained values of n were in the range 0.2 to 0.3.

De Gennes [111] and Cazabat [57] derived power law from a balance of forces that drive and resist spreading. In a general way the kinetic equation can be written as:

$$R \propto V^m t^n \tag{35}$$

Where

m= 0.3 for small drops and 0.375 for large drops
n= 0.1 for small drops and 0.125 for large drops

Lavi and Marmur investigated the partial spreading of organic liquids on coated silicon wafer [1]. Exponential power law (given below) was successfully used to show the partial spreading kinetics in their experiments.

$$\frac{A}{A_f} = 1 - \exp\left(-\frac{K}{A_f}\tau^n\right) \tag{36}$$

where A is the measured liquid–solid contact area (normalized with respect to $(V)^{2/3}$), A_f is the final, equilibrium value of the normalized wet area, τ is the dimensionless time (equal to $\gamma t/(\mu V^{1/3})$, t is the time, K and n are empirical constants, V is drop volume, γ is the liquid surface tension and μ is the liquid viscosity. The linear decrease of parameter K with the ratio (μ/γ) was also observed indicating quicker kinetics at lower viscosities and higher surface tensions. The capillary number, Ca, was also found out by transforming exponential power law and observed satisfactory fitting of the empirical relation at high as well as low capillary numbers.

5.2. Reactive systems

If there is a reaction/diffusion in the system, then its effect also has to be taken into account while analyzing the kinetics of spreading. The spreading of solder on a substrate, wetting of ceramic substrate by a molten metal, etc. are generally involved with a chemical reaction between the spreading liquid and active substrate components.

A wide diversity of processes such as diffusion, chemical reaction and fluxing and their possible combinations affect not only the extent of wetting but also moderate the wetting rate. In real reactive systems, a single function can hardly describe the full range of relaxation behaviour which actually results from the action of several different phenomena. Hence, different rate laws should be expected for kinetics of reactive wetting depending on the controlling processes. Reactive wetting and spreading with solidification in various systems have been studied, analyzed and modeled by various researchers [2,10,17,31,40,68,74,77,78,91,92,94–99,112,113].

Five stages are identified in a reactive wetting: (i) an initial rapid spreading stage, (ii) an initial quasi equilibrium stage, (iii) an interfacial front advancing stage, (iv) no advancing but continuous decrease in drop height stage and (v) a final wetting equilibrium stage. The rapid spreading stage is similar to the non-reactive wetting and can generally be explained by Young's equation. However, no theoretical models are developed to describe complete reactive wetting phenomenon. Only empirical relations are used in which best fit equations are suggested for the experimental results.

Lopez and Kennedy investigated the flux assisted spreading in a reactive system of Al/TiC at inert as well as general air environments [10]. The use of flux has the potential to make the surrounding atmosphere a non-critical one since their observations indicated that in the presence of flux, the wetting behaviour becomes much less sensitive to temperature, the cleanliness of the droplet as well as substrate surfaces and the gaseous environment.

Shen et al. investigated the reactive wetting of high purity vitreous SiO_2 substrates by molten aluminium using sessile drop technique [74]. A very important observation made by them—significant decrease of drop height with negligible increase in drop base diameter—a common feature of most reactive systems. Hence, to assess the wetting behaviour it is necessary to take into account the variations in drop height and base diameter in addition to decrease in contact angle. All the five stages of a reactive wetting are identified. A decrease in contact angle may be due to: (i) advancing interface (an improvement in wetting) or (ii) consumption of spreading liquid by reaction with active substrate (no improvement in wetting). Hence, in reactive wetting systems the true wetting improvement must satisfy the conditions of $d\theta/dt < 0$ and $dD/dt > 0$, where θ is the dynamic contact angle and D is the dynamic drop base diameter.

The rate-limiting steps controlling the spreading of solder on metal surfaces are [68]:

- The reaction of the solder with the substrate to form intermetallic compounds.
- The reaction and removal of surface contaminants by the solder flux.

Peebles et al. carried out investigations on the spreading of pure tin on copper substrates to study the spreading kinetics and its temperature dependence [68]. The ratio R/R_o was used as spreading parameter where R is the measured radius of spreading drop and R_o is the radius of the drop when contact angle is 90°. Hence, R_o can be determined as follows by assuming a hemi-spherical geometry:

$$R_o = \left[\frac{3m}{2\pi\rho}\right]^{1/3} \tag{37}$$

where m and ρ represent mass and density of solder drop.

Their observations indicated that the solder spreading is a thermally activated process. The spreading rates $\left(\frac{\mathrm{d}}{\mathrm{d}t}\left(\frac{R}{R_o}\right)\right)$ increased rapidly with increasing temperatures. The order of spreading n was determined for the spreading of tin. The spreading followed $t^{1/3}$ kinetics up to 327 °C and $t^{1/5}$ thereafter. They also found that the mechanism of spreading dramatically changed at 327 °C. The spreading was thermally activated till that temperature and became thermally non-activated at any higher temperatures (Fig. 30). To investigate the causes for this change surface chemistry studies were carried out on the substrate in the same temperature range. The removal of the surface oxide might be the rate limiting step for the solder spreading below 327 °C where as the decomposition of the surface Cu_2O at and above 330 °C resulted in the generation of cleaner surface that allowed pure Sn to spread more rapidly.

Kang et al. observed that the rate at which contact angle decreases and the triple line velocity ($\mathrm{d}R/\mathrm{d}t$) increases were dependent not only on time but also on temperature [30]. In order to analyze the wetting, a reflow process parameter, known as duration time (t_d), has been proposed. It is the time required for the contact angle to evolve from 140° to 50°. A reduction up to 70% has been observed in their experiments when temperature is increased from 190° to 230°. The effect of surface metallization has also been studied by comparing the wetting on surfaces with Cu and Ni finish. Due to slower reaction between the Ni layer and molten solder, contact angle reduction is slower on a surface with Ni finish when compared with that on a surface with Cu finish. The isothermal spreading of liquid Sn on Au substrates had been studied by Singler et al. [77]. Sessile drop spreading in the temperature range of 250–430 °C was recorded digitally in their experiments. Limited spreading was observed at lower temperatures whereas spreading rates accelerated as the temperatures were increased. Extensive spreading was observed at higher temperatures and liquid Sn exhibited perfect wetting on Au at 430 °C.

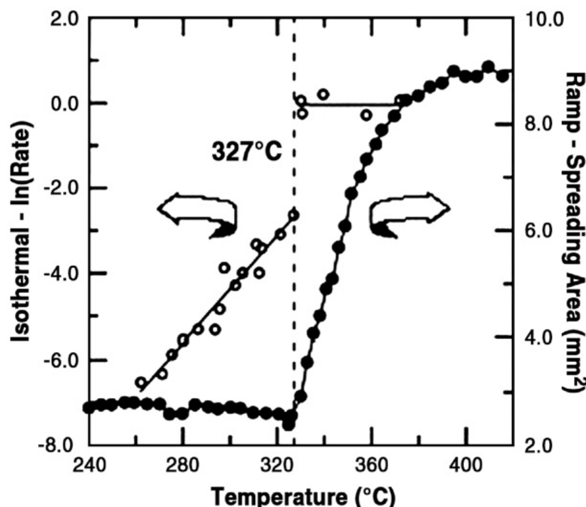

Fig. 30. Change of spreading mechanism at elevated temperature [68].

Eustathopoulos et al. [17,78,94–98] investigated the dynamics of wetting in metal/ceramic reactive systems in detail. The driving force for the reactive wetting is identified as:

$$F_d(t) = \gamma^o_{LV}(\cos\theta_P - \cos\theta(t)) \tag{38}$$

where θ_P is the equilibrium contact angle of the liquid on the reaction product surface.

It is also clear from the comparison of wetting times that the spreading rate is not controlled by viscous resistance (as in the case of inert systems). In non-reactive spreading, the capillary equilibrium is generally achieved in fraction of a second where as in during wetting of a substrate by a liquid metal the corresponding time (10 to 10,000 s) is several order magnitudes larger than this. Hence, in reactive systems, the rate of spreading is controlled not by viscous resistance but by interfacial reaction itself [17]. As a consequence, the spreading in a reactive system is a 2-stage process as pointed below:

- Local process at the interface and
- Transport phenomena in the bulk material

Here, two limiting cases arise depending on the rate of chemical reaction at the triple line compared to the rate of diffusion of reactive solute from the drop bulk to the triple line. One, the chemical kinetics at the triple line is rate-limiting since the diffusion within the droplet is comparatively rapid and the other, the transport (diffusion and convection) is rate limiting as the local reaction rates are comparatively rapid. Hence, it is difficult to explain the entire behaviour by a single kinetic equation as mentioned earlier.

Various kinetic equations found in the literature are summarized in Table 7.

6. Modeling of spreading

Modeling of spreading behaviour needs basic understanding of the forces acting on a spreading drop. The problem of

Table 7
Spreading kinetics

Kinetic equation	Comment	Reference
$\left[\frac{A}{V^{2/3}}\right] = Ct^n$ and $C \propto V^{2/3}$	Experimental observation; volume effect is taken into account	[114]
$\cos\theta_d = \cos\theta_e [1 - A * \exp(-ct)]$	Correlation with experimental results	[114]
$R \sim t^{1/10}$	Theoretical derivation	[111]
$\theta_t - \theta_f = (\theta_o - \theta_f)\exp(-t/\tau)$	Fitting the curve to experimental data	[94]
$\cos\theta_f - \cos\theta_t = A\exp(-Ct)$	Fitting the curve to experimental data	[94]
$r(t) \approx t$	Experimental observation	[115]
$r(t) = \sqrt{t}$	Experimental observation	[115]
$r(t) \approx \exp(t)$	Experimental observation	[115]

modeling the phenomenon is generally treated by taking one or more of the following approaches:

- Dependence of the driving force on the difference between the dynamic and equilibrium contact angles.
- The effective energy dissipation channel during spreading

Initial models developed were dependent either on empirical expressions or fitting to the experimental observations. In these models physical aspects were given importance rather than thermodynamic aspects [65,114,116–119].

6.1. Model for complete spreading

In inert systems models for complete spreading are developed on theoretical basis by considering various forces that drive and resist spreading. Consider the spontaneous spreading of a sessile drop on an ideal surface. There are two forces that drive spreading:

- Capillary or surface tension force
- Gravity force

On the other hand on an ideal surface the force that opposes spreading is the viscous force.

Using the terminology given in the figure, the capillary force can be approximated by

$$F_c = \gamma\theta^2 \qquad (39)$$

and gravity force can be approximated by

$$F_g = h^2\rho g \qquad (40)$$

Similarly viscous force can be approximated by

$$F_v = \mu UR/h \qquad (41)$$

Here θ is the contact angle (which can be approximated to the ratio of h to R by assuming spherical cap drop shape and constant volume), h is the apex height of the drop from the base and R is the drop base radius, all three are dynamic or instantaneous quantities. U represents the contact line velocity (given by dR/dt). ρ, γ and μ represent density, surface tension and viscosity of the spreading liquid respectively.

It is reasonable to neglect the effect of gravity for small drops and the effect of surface tension for large drops. Under this assumption, equating driving and resisting forces and carrying out necessary manipulations yield:

$$R \propto t^n \qquad (42)$$

where the value of n is 0.1 or 0.125 for small or large drops respectively. The above relation is generally known as Tanner's law.

6.2. The hydrodynamic model

Two basic but different approaches exist to describe the partial spreading of a drop: hydrodynamics and molecular kinetics. It is agreeable that the liquid–solid system dissipates energy during spreading since the shape of the drop changes with time. The above two approaches differ from each other in the consideration of effective dissipation channel [101].

In the hydrodynamic model, the dissipation is mainly due to the viscous flows generated in the core of the spreading droplet (Fig. 31). The key features of the model can be listed as follows [31,73,101,111,116,121]:

- The prime assumption is that the spreading process is dominated by viscous dissipation of the liquid. (In other words, the bulk viscosity or viscous friction is the main resistance for the motion of the three-phase contact line.)
- The molecular dissipation at the tip is negligible.
- The spreading liquid is separated into (at least) two regions-inner core and outer region.
- The model does not take into account the characteristics of the solid surface. (This is a serious limitation of the model.)

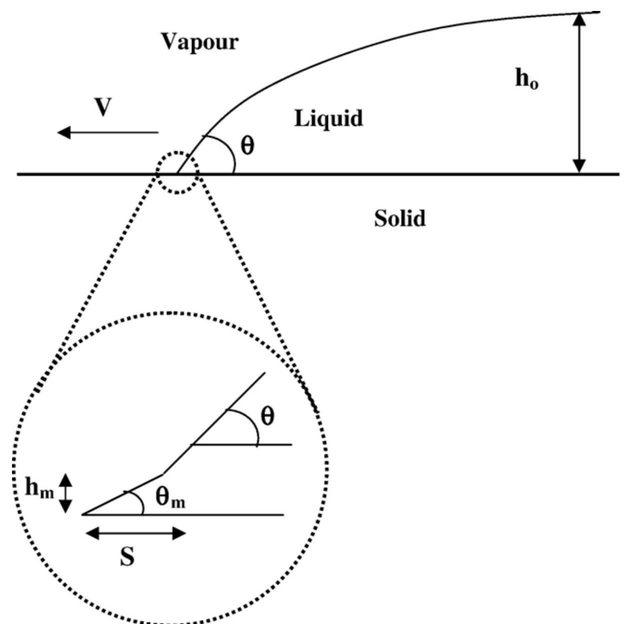

Fig. 31. The hydrodynamic model [120].

- The velocity dependence of contact angle is given by:

$$\theta^3 = \theta_o^3 \pm 9 \frac{\mu V}{\gamma_{lv}} \ln(L/L_s) \tag{43}$$

where L is the capillary length $= \sqrt{\frac{2\gamma_{lv}}{\rho g}}$
L_s is the fitting parameter, known as slip length
V is the velocity of the contact line

- Rearrangement of terms will give the expression for wetting velocity:

$$v = \gamma_{lv} \left[\frac{\theta^3 - \theta_o^3}{9\mu \ln(L/L_s)} \right] \tag{44}$$

It was shown by number of researchers that drop base radius (R) grows with time (t) according to $R \sim t^{1/10}$ or the contact angle (θ) decreases with time as $\theta \sim t^{-3/10}$. Further, in this approach, a limiting height (L_s) is defined below which the approach ceases to act and this cut-off height is assumed to be in the order of 10^{-9} to 10^{-8} m. There are few important disadvantages in the model. First, the model fails to demonstrate the behaviour of low viscosity fluids. Second, the model predicts very small and unrealistic values for limiting height (in the order of molecular dimensions). Third, it does not take into account the substrate surface characteristics.

6.3. The molecular kinetic model

In the molecular kinetic model, the dissipation is mainly due to adsorption or attachment of fluid particles to the solid (Fig. 32). The model predicts the time dependence of drop base radius and contact angle according to: $R \sim t^{1/7}$ and $\theta \sim t^{-3/7}$.

The key features of the model can be enumerated as follows [31,73,101,111,116,121]:

- The prime assumption is that energy dissipation occurs only at the moving contact line. Therefore, the contact line velocity is controlled by adsorption/desorption processes very near the contact line.
- The model excludes any viscous dissipation taking place.
- The solid surface characteristics are taken into account. As a result, the molecules which are in direct contact with the solid become important and the last such molecule will tend to hop from one absorption site to the next and it may return also.
- The rate at which hopping takes place is given by:

$$K_{\pm} = k \exp \left[- \frac{W \pm \frac{1}{2} F \lambda^2}{k_B T} \right] \tag{45}$$

where W is the activation energy for hopping, λ is the distance between hopping sites, F is the force per unit length.

- Hence, the net contact line velocity is given by: $v = \lambda(K+ - K-)$
- The velocity dependence of contact angle is given by:

$$\cos\theta = \cos\theta_o \pm \frac{2kT}{\gamma_{lv}\lambda^2} \sinh^{-1} \left(\frac{V}{2K_w \lambda} \right) \tag{46}$$

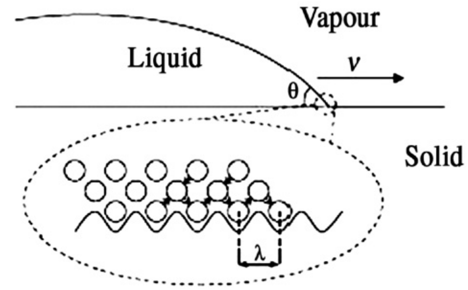

Fig. 32. The molecular kinetic model [120].

where k is the Boltzman constant, λ and K_w are the fitting parameters (physically represent the distance between two adsorption/desorption sites and quasi-equilibrium rate constant).

- Rearranging the terms results in the expression for wetting velocity.

$$v = 2K_{eq} \lambda \sinh \left[\frac{\gamma_{lv}(\cos\theta_o - \cos\theta)}{2nk_B T} \right] \tag{47}$$

Here n represents the number absorption/desorption sites per unit area.

6.4. Combined models

Combined theories have also been proposed since in a real situation, both types of dissipation effects are generally present. According to de Gennes the molecular features are important at high velocities and large angles whereas for low angles and when the displaced phase is more viscous than the displacing phase, the hydrodynamic approach would be essential [111].

The simple way to do this is to add a viscous contribution to the barriers created by the liquid/solid attractions [101]. However this procedure failed to match with experimental results. Under complete wetting conditions, de Gennes suggested that the unbalanced capillary force should be compensated by a total energy dissipation occurring during the spreading process. The total dissipated energy consists of viscous dissipation in the core of the drop, dissipation at the advancing contact line and that in the precursor film. The frictional energy dissipation taking place at the solid/liquid interface has been neglected and dissipation in the precursor film is given importance in this model [101,111].

The various theories were applied to the experimental data to explain the temperature dependence of contact angle [72]. The molecular kinetic model was able to explain the dynamic contact angle behaviour at different temperatures. However, the model failed to explain the weak dependence of the free activation energy of wetting on the temperature. On the other hand, the experimental data could fit with hydrodynamic model but could not provide physically meaningful parameters. Another important point they identified is that both models emphasize only one type of dissipation (Molecular kinetic-adsorption; hydrodynamic-viscous flow) and fail to account for the total dissipation. Hence, De Coninck et al. followed a

standard mechanical approach to describe the time evolution of the drop in which the driving force (i.e., the increase in drop free energy due to the increase in base radius) is balanced by the rate of total dissipation. This combined model predicts a behaviour in which a hydrodynamic regime is preceded by a molecular kinetic regime [101].

6.5. Frenkel's approach

Frenkel's approach of determining equilibrium contact angle of a spherical cap droplet using the change in surface energy with evolution of the drop is modified and applied to dynamic wetting by McHale and Newton [65]. Basically the technique uses the principles of hydrodynamic approach. The rate of change of surface free energy of a given drop shape is equated to the rate of viscous dissipation inside the drop. The key feature of the model is that it can be applied to both rough (regular) and heterogeneous surfaces.

The rate of change of surface free energy is given by:

- $$\frac{dF}{dt} = 2\pi\gamma_{lv}[\cos\theta - I]r_o v_E \quad \text{for a smooth surface} \tag{48}$$
- $$\frac{dF}{dt} = 2\pi\gamma_{lv}[\cos\theta - rI]r_o v_E \quad \text{for a rough surface} \tag{49}$$
- $$\frac{dF}{dt} = 2\pi\gamma_{lv}[\cos\theta - frI + g]r_o v_E \tag{50}$$
  for a rough surface with trapped vapour
- $$\frac{dF}{dt} = 2\pi\gamma_{lv}[\cos\theta - fI_1 - (1-f)I_2]r_o v_E \tag{51}$$
  for a heterogeneous surface

where θ is the contact angler_o is the base radius

$$I = \frac{\gamma_{SV} - \gamma_{SL}}{\gamma_{LV}}$$

edge speed, $v_E = \frac{-(3V/\pi)^{1/3}d\theta/dt}{(1-\cos\theta)^{2/3}(2+\cos\theta)^{4/3}}$$r$ is the geometric roughness factor ($=\Delta A_{True}/\Delta A$)$f$ and g are the fractions of rough surface covered by liquid and vapour.

To determine the viscous dissipation, a cone is assumed within the spherical cap. Assuming Poiseuille flow within the cone, the rate energy dissipation is given by:

$$\frac{dE_d}{dt} = \frac{8\pi\eta v_E^2 r_o J_W}{3\tan(\theta/2)} \tag{52}$$

where η is the viscosity of the liquid$\tan(\theta/2)$ is the ratio of cap height to contact radius $J_W=\varepsilon-\ln\ \varepsilon-1\varepsilon$ is the cut-off parameter.

By equating the rate of change of surface free energy with the rate of change of viscous dissipation, a relation between edge-speed and contact angle can be obtained and it can be used to model the spreading behaviour. McHale and Newton [65] showed that the approach would result into Tanner's results.

6.6. Overall energy balance approach

Gu and Li developed a model for spreading based on overall energy balance [117, 118]. It was proposed that the spreading process of a liquid drop can be described by the overall energy balance (OEB) equation as follows:

$$\frac{d}{dt}[E_k(t) + E_p(t) + E_g(t)] + \frac{dL_f(t)}{dt} = 0 \tag{53}$$

where the three terms inside the first square bracket respectively represent kinetic energy, potential energy due to interfacial tensions and potential energy due to gravity where as the second term represents the power of energy dissipation. Each of these terms can be evaluated as follows:

- $E_k(t) = \frac{1}{2}mU_m^2$ where m is the mass of the liquid drop and U_m is the speed of the mass center point of the liquid drop which can be determined from the position of mass center point at various time instances.
- $E_p(t)=\gamma_{lf}\ [A_{sl}(t)-A_{sl}(t)\cos\ \theta_e]+\gamma_{lf}\ A_{sf}A_{total}$ where γ has its usual meaning.
- $E_p(t)=mgy_m(t)$ where y_m is the vertical position of the mass center point.
- $L_f(t) = 6\pi\mu\ln(\varepsilon^{-1})\int_0^t \frac{R(t)}{\theta(t)}\left[\frac{dR(t)}{dt}\right]^2 dt$ where μ is the liquid viscosity and ε is adjustable parameter.

Integration of overall energy balance equation with respect to time from $t=0$ to any time t will yield the general OEB equation that can be used to model the spreading of a liquid drop on a horizontal solid substrate. To determine the drop shape profile Laplace equation of capillarity can be used.

The model combines both physical and fluid mechanics aspects of drop spreading. All the observed effects such as inertia, viscous, gravity, interfacial tensions, etc. are taken into account in the model. However, numerical methods have to be followed to solve the OEB equation.

6.7. Model for spreading on rough surface

The model developed by Marmur and Apel-Paz [64] is of particular interest for spreading on rough surfaces. The spreading of liquids on practical rough surfaces occurs by two modes (Fig. 33):

- On the top of the rough surface
- Inside the capillary grooves (formation of the rim)

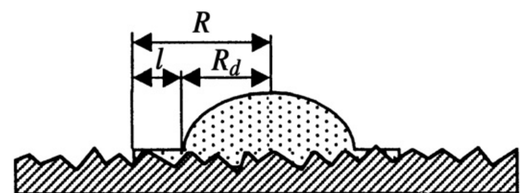

Fig. 33. Two modes of spreading on a rough surface [64].

As shown in the figure, R_d is the base radius and l is the rim length. Hence, the radius of outer edge of the rim, R, is given by:

$$R = R_d + 1 \quad (54)$$

Assuming that the spreading follows a power law:

$$A = \pi R_d^2 = k(t + \tau)^n \quad (55)$$

where

A is the wetted area under the drop
t is the time
k and n are the empirical constants
τ is the measure of uncertainty in defining zero time.

At time, $t=0$, with the drop already wet the solid,

$$A_o = \pi R_{do}^2 = k\tau^n \quad (56)$$

Marmur assumed that a capillary is attached to the drop (to simulate the roughness grooves). The capillary is fed by the edge of the drop, which continues to spread simultaneously with the penetration of the liquid into the grooves. Hence, the location of the entrance to the capillary is moving with the time.

6.8. Models for spreading in reactive systems

In non-reactive systems, the spreading rate is controlled by the viscous flow and described by a power function of drop base radius, R versus time, t, for angles less than 60° [17]:

$$R^n \approx t \quad (57)$$

where n is found to be 10.

On other hand, a reactive wetting kinetics is affected by number of processes such as diffusion, convection, deoxidation, interfacial reaction, etc. It is difficult to develop a theoretical model for the spreading process. Hence, earlier efforts consists of fitting experimental $\theta(t)$ or $R(t)$ relaxation curves by different functions. Some of the empirical models found in the literature are summarized in the Table 8.

Table 8
Models of spreading

Model	Comment	Reference
$\tan\theta_d = [\tan^3\theta_e - 9\log\eta Ca]^{1/3}$ where η is Hamaker constant and Ca is capillary number	Semi-empirical equation (Precursor film model)	[118]
$v_E \propto \theta^3$ where v_E is edge speed	Complete wetting (Tanner's law)	[65]
$v_E \propto \theta(\theta^2 - \theta_e^2)$	Partial wetting (Modified Tanner's law	[65]
$\theta \propto (t+C)^{-3/10}$ where C is a constant	Drop size ≪ capillary length Surface is smooth Spherical cap drop shape	[65]
$\theta \propto (t+C)^{-3/4}$	Rough surface	[65]
$\theta_D^3 - \theta_m^3 = 9Ca\ln\left(\frac{L}{L_m}\right)$ for $\theta_m = \theta_s; \theta_D < 3\pi/4$	Hydrodynamic approach	[119]
$R(t) \sim t^{1/10}; \theta_D(t) \sim t^{3/10}$	Hydrodynamic model, small drops	[119]
$u = \frac{k^o \lambda^3 \gamma(\cos\theta_s - \cos\theta_D)}{k_B T}$	Molecular kinetic approach	[119]
$R(t) \sim t^{1/7}; \theta_D(t) \sim t^{3/7}$	Combined approach	[119]
$\frac{d}{dt}(\cos\theta_d) = \frac{\sigma xy}{CV}(\cos\theta_e - \cos\theta_d)$	Eyring's approach of absolute reaction rates	[114]
$A_t = K^2(\sigma V^3/\mu)^{0.2} t_e^{0.2}$ where $K^2 = \left(\frac{640\pi^2}{3B^3}\right)^{0.2}$	Lubrication theory Flat and smooth surface, Newtonian and non-volatile liquid. Gravity and inertia effects are neglected	[122]
$\theta(t) = 82.64BCa^{1/3}$	–	[122]
$R \approx V^{3/10}[\gamma t/\mu]^{1/3}$	Small drops	[57]
$R \approx V^{3/8}[\rho\gamma t/\mu]^{1/8}$	Large drops	[57]
$v = \frac{\gamma_{lv}}{\mu}\frac{x^2 y}{V_h}(\cos\theta_{eq} - \cos\theta_d)$	–	[8]
$v_o = \frac{\pi(r(t))^3}{6}\tan[\theta(t)/2][3 + \tan^2(\theta(t)/2)]$	–	[111]
$\cdot r(t) = \mu[1 - C_e/C_o]$	Reaction controlled wetting	[111]
$\cdot r(t) = \frac{2D}{r(t)}\left[\frac{C_o}{C_e} - 1\right]F(t)\sin\theta(t)$ where $F(t) = \sum_{n=1}^{\infty}\exp(D\lambda_n^2 t)$	Diffusion controlled wetting	[111]
$v = 2\kappa_{eq}\lambda\sinh\left[\frac{\gamma_{lv}(\cos\theta_{eq} - \cos\theta)}{2nk_B T}\right]$	Molecular kinetic approach Gravity and chemical reaction neglected	[73]
$v = \gamma_{lv}\frac{\theta^3 - \theta_{eq}^3}{9\mu\ln(r/s)}$	Hydrodynamic approach Gravity and chemical reaction neglected	[73]
$R - R_o = Kt$	Reaction-limited spreading	[94]
$R^4 - R_o^4 = Kt$	Diffusion-limited spreading	[94]

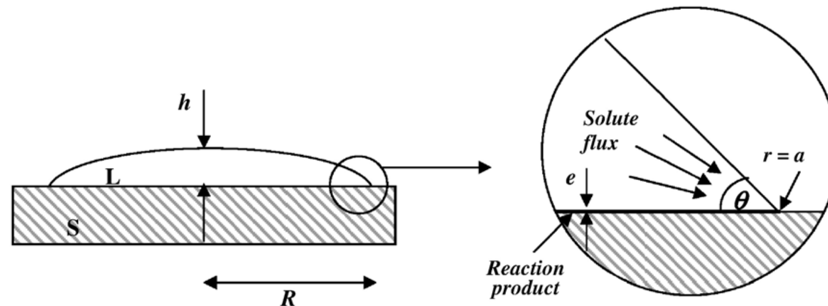

Fig. 34. Two models of spreading on a rough surface [78,95,96].

Eustathopoulos et al. attempted to develop a model, known as reaction product control (RPC) model for the reactive metal/ ceramic system after extensive experimental investigation of number of reactive systems [17,78,94–99]. The important features of the model are:

- In a reactive system, the spreading kinetics is mainly guided by chemical reactions taking place at the triple line interface and transport of reactive species from the drop bulk to the triple line.
- Two limiting cases in the above configuration are reaction-limited spreading and transport-limited spreading.
- In the reaction limited spreading, the chemical kinetics at the triple line is rate controlling since the diffusion within the droplet is comparatively rapid. It may be noted that the diffusion is not at all required if the drop is made of a reactive metal.
- It is assumed that the reaction does not change the global drop composition significantly and a steady configuration is established at the triple line during wetting.
- With above assumptions, the rate of reaction and hence the triple line velocity is constant with time:

$$R - R_o = Kt \tag{58}$$

  where K is a constant independent of drop volume.
- This linear spreading is observed in number of cases after initial drop spreading
- When the local reaction rates are comparably rapid and the extent of local reaction which drives spreading is limited by the diffusive supply of reactants from the drop bulk to the triple line, the transport-limited spreading results (Fig. 34).
- If the controlling process is pure diffusion, a simple diffusion model which neglects convection in drop and reaction at the interface yields following kinetic equation:

$$R^4 - R_o^4 = KVt \tag{59}$$

  where V is the drop volume and K is a constant.
- On the other hand, the convection within the drop is taken into account, the model has to be modified. Based on Marangoni convection in liquids, the following model is proposed:

$$R^{5.5} - R_o^{5.5} = \alpha t \tag{60}$$

  where α is the proportionality constant.

However, complete modeling of the reactive wetting process, should include, an additional term to account for interfacial reactions.

7. Summary

Wetting of liquids on surfaces is a complex phenomenon and is of great technological importance since large number of industrial processes involve wetting. The two important parameters to characterize the wetting are the degree and the rate of wetting. Contact angle is a measure of the degree of wetting or wettability of a surface by a liquid. The greatest difficulty in studying the wetting behaviour is obtaining reproducible results. This is mainly due to the sensitivity of the contact angle and hence wetting to large number of factors discussed. Various methods have been developed over the years to evaluate wettability of a solid by a liquid. Among these, sessile drop and wetting balance techniques are versatile, popular and provide reliable data.

Young's equation gives the basic mathematical formulation of contact angle in terms of surface and interfacial tensions. A variety of contact angles has been defined to address different situations arising due the sensitivity of contact angle to a great number of factors. The important factors that affect the wetting behaviour of a liquid on a solid are substrate surface roughness and heterogeneity, temperature of the system, atmosphere, flux, properties of the spreading liquid, trace impurity/alloying addition, etc. Wenzel's and Cassie's laws are generally used to account for roughness and heterogeneity of the substrate surface. The effect of temperature is generally studied by measuring the activation energy for spreading. Contradicting results exist about the effect of various factors.

The thermodynamic treatment of the contact angle/wetting in an inert system is mainly governed by surface free energies where as that in the reactive system depends on interfacial reaction and factors affecting it. Satisfactory theoretical explanations are found for the non-reactive spreading kinetics and successful theoretical models are also developed. Classical models for spreading kinetics in inert systems account for surface tension and gravity as driving and viscous dissipation as restraining forces. The assumption is that the substrate is not only inert but also smooth and homogeneous. These models are further extended to real surfaces. However, in real reactive systems, a single function can hardly describe the full range of relaxation behaviour which actually results from the action of

several different phenomena. Different flow patterns exist at different stages.

Spreading kinetics in a given system is strongly affected by the experimental conditions. The same system exhibits different kinetic patterns under different conditions. Hence it is quite difficult to understand the underlying mechanism and suggest a suitable mathematical model to describe the kinetics of spreading. In reactive systems, wetting and chemical interfacial reactions are interrelated and hence for successful modeling it is essential to couple interfacial reactions as well as factors affecting these reactions with kinetics of wetting. The effect of interfacial reactions, diffusion of constituents, dissolution of substrate on the evolution of contact angle and wetting kinetics needs to be investigated and quantified.

References

[1] Lavi B, Marmur A. Colloids Surf A 2004;250:409–14.
[2] Bhola R, Chandra S. J Mater Sci 1999;34:4883–94.
[3] Manko HH. Solders and soldering. 3rd Edition. NY: McGraw-Hill Inc.; 1992. p. 1–153.
[4] Frear DR, Jones WB, Kinsman KR. Solder mechanics—a state of the art assessment. A TMS Publication; 1991. p. 1–104.
[5] He B, Lee J, Patankar NA. Colloids Surf A 2004;248:101–4.
[6] Kijlstra J, Reihs K, Klamt A. Colloids Surf A 2002;206:521–9.
[7] Lee CC, Kim J. IEEE 2005; 0-7803-9085-7/05.
[8] Schwartz AM, Tejada SB. J Colloid Interface Sci 1972;38–2:359–75.
[9] Vianco PT, Frear DR. JOM July 1993:14–9.
[10] Lopez VH, Kennedy AR. J Colloid Interface Sci 2006;298–1:356–62.
[11] Schwartz MM, Aircraft S. Metals hand book, 10th edition, vol. 6. Metals Park, OH: ASM; 1991. p. 126–9.
[12] Bernardin JD, Mudawar I, Walsh CB, Franses I. Int J Heat Mass Transfer 1997;40–5:1017–33.
[13] Sefiane K, Tadrist L, Douglas M. Int J Heat Mass Transfer 2003;46: 4527–34.
[14] Chandra S, di Marzo M, Qiao YM, Tartarini P. Fire Safety J 1996;27: 141–58.
[15] Adamson AW, Gast AP. Physical chemistry of surfaces. 6th Ed. New York: Wiley-Interscience; 1997. p. 347–79.
[16] Long J, Hyder MN, Huang RYM, Chen P. Adv Colloid Interface Sci 2005;118:173–6.
[17] Eustathopoulos N. Acta Mater 1998;46–7:2319–27.
[18] Morra M, Occhiello E, Garbassi F. Adv Colloid Interface Sci 1990;32: 79–116.
[19] Davis JT, Rideal EK. Interfacial phenomena. 2nd Edition. NY: Academic Press; 1966. p. 1–52.
[20] Quere D. Physica A 2002;313:32–46.
[21] Yoon SW, Choi WK, Lee HM. Scripta Mater 1999;40–3:297–302.
[22] Sauer BB, Kampert WG. J Colloid Interface Sci 1998;199:28–37.
[23] Zengerle R. (http://www.imtek.de/anwendungen/content/vorlesung/2005/mikrofluidik_i_5_-_surfacetension.pdf).
[24] Lam CNC, Kim N, Hui D, Kwok DY, Hair ML, Neumann AW. Colloids Surf A 2001;189:265–78.
[25] Bukat K, Sitek J, Hozu L, Bulwith R. Global SMT and Packaging Journal; December 2002. p. 1–8.
[26] Takao H, Tsukada T, Yamada K, Yamashita M, Hasegawa H. R & D Review of Toyota CRDL; 39–2:41–8.
[27] Hong SM, Park JY, Kang CS, Jung JP. IEEE Trans Comp Pack Techn 2003;26–1:255–61.
[28] Mackie AC. Circuits Assembly March 2003:26–35.
[29] Yu DQ, Zhao J, Wang L. J Alloys Compd 2004;76:170–5.
[30] Kang SC, Kim C, Muncy J, Schmidt M, Baldwin D. IEEE/SEMI International Electronics Manufacturing Technology Symposium; 2004.
[31] Saiz E, Hwang CW, Suganuma K, Tomsia AP. Acta Mater 2003;51: 3185–97.
[32] Yu DQ, Xie HP, Wang L. J Alloys Compd 2004;385:119–25.
[33] Lin CT, Lin KL. Appl Surf Sci 2003;214:243–58.
[34] Wang H, Wang F, Gao F, Ma X, Qian Y. J Alloys Compd 2007;433–1 (2):302–5.
[35] Marmur A. Adv Colloid Interface Sci 1994;50:121–41.
[36] Marmur A. Colloids Surf A 1996;116:55–61.
[37] Bonn D, Eggers J, Meunier J, Rolley E. (http://www.maths.bris.ac.uk/~majge/rmp) p. 8.
[38] Kandlikar SG, Steinke ME. Int J Heat Mass Transfer 2002;45:3771–80.
[39] Extrand CW, Kumagai YJ. Colloid Interface Sci 1997;191:378–83.
[40] Kamusewitz H, Possart W, Paul D. Colloids Surf A 1999;156:271–9.
[41] Plas HAV, Cinque RB, Mei Z, Holder H. Hewlett-Packard J 1997:1–7.
[42] Yost FG, Michael JR, Eisenmann ET. Acta metal 1995;43–1:299–305.
[43] Woodward RP. (http://www.firsttenangstroms.com) p. 1–8.
[44] Martorano KM, Martorano MA, Brandi SD. Engenharia Metalugica/USP-2004:1–14.
[45] Sattiraju SV, Dang B, Johnson RW, Li Y, Smith JS, Bozack MJ. IEEE Trans Electron Packag Manuf July 2002;25–3:168–84.
[46] Yu DQ, Wang L, Wu CML, Law CMT. J Alloys Compd 2005;389–1,2: 153–8.
[47] Solomon HD, Delair RE, Thyssen J. Weld Res October 2003:278–87.
[48] Yasuda K, Akamizu H, Fujimoto K, Nakata S. IEEE/CPMT International Electronics Manufacturing Technology Symposium; 2000. p. 247–52.
[49] Awasthi A, Bhatt YJ, Garg SP. Meas Sci Technol 1996;7:753–7.
[50] Shibata H, Jiang X, Valdez M, Cramb AW. Met Mat Trans B 2004;35: 179–80.
[51] Wolansky G, Marmur A. Colloids Surf A 1999;156:381–8.
[52] Nakae H, Inui R, Hirata Y, Saito H. Acta Mater 1998;46–7:2313–8.
[53] Sakai H, Fujii T. J Colloid Interface Sci 1999;210:152–6.
[54] Shuttleworth R, Bailey GLJ. Disc Faraday Soc 1948;3:16.
[55] Uelzen T, Muller J. Thin Solid Films 2003;434:311–5.
[56] Hitchcock SJ, Carroll NT, Nicholas MG. J Mater Sci 1981;16:714.
[57] Cazabat AM, Stuart MAC. J Phys Chem 1986;90:5845–9.
[58] Volpe CD, Maqniglio D, Morra M, Siboni S. Colloids Surf A 2002;206: 47–67.
[59] Sikalo S, Marengo M, Tropea C, Ganic EN. Exp Ther Fluid Sci 2002;25: 503–10.
[60] Li WT, Charters RB, Davies BL, Mar L. Appl Surf Sci 2004;233: 227–33.
[61] Takata Y, Hidaka S, Yamashita A, Yamamoto H. Int J Heat Fluid Flow 2004;25:320–8.
[62] Callewaert M, Gohy JF, Gillain CCD, Petermann LB, Rouxhet PG. Surf Sci 2005;575:125–35.
[63] Nicholas MG, Crispin RM. J Mater Sci 1986;21:522.
[64] Apel-Paz M, Marmur A. Colloids Surf A 1999;146:273–9.
[65] McHale G, Newton ML. Colloids Surf A 2002;206:193–201.
[66] Claesson E, Choquenet L, Nilson M, Brasage — 97.
[67] Vaynman S, Fine ME. Scripta Mater 1999;41–12:1269–71.
[68] Peebles DE, Peebles HC, Ohlhausen JA. Colloids Surf A 1998;144: 89–114.
[69] Wu CML, Yu DQ, Law CMT, Wang L. Mater Sci Eng R 2004;44: 1–44.
[70] Farooq M, Ray S, Sarkhel A, Goldsmith C. Electronic Components and Technology Conference; 2001. p. 978–86.
[71] Abtew M, Selvaduray G. Mater Sci Eng R 2000;27:95–141.
[72] de Ruijter M, Kolsh P, Voue M, De Coninck J, Rabe JP. Colloids Surf A 1998;144:235–43.
[73] Kang SC, Baldwin DF. 8th Int Symp Adv Pack Mat IEEE; 2002. p. 47–53.
[74] Shen P, Fujii H, Matsumoto T, Nogi K. Met Mat Trans A 2004;35A: 583–8.
[75] Fujiuchi S. 11th IEEE/CHMT International Electronics Manufacturing Technology Symposium; 1991. p. 163–5.
[76] Kitajima M, Shono T. Microelectron Reliab 2005;45–7,8:1208–14.
[77] Yin L, Meschter SJ, Singler TJ. Acta Mater 2004;52:2873–88.
[78] Mortensen A, Drevet B, Eustathopoulos N. Scripta Mater 1997;36–6: 645–51.
[79] Chen K, Lin KL. International Symposium on Electronic Materials and Packaging; 2002. p. 49–54.
[80] Wang L, Yu DQ, Zhao J, Huang ML. Mater Lett 2002;56:1039–42.

[81] Suganuma K, Muata T, Noguchi H, Toyoda Y. J Mater Res 2000;15–4: 884–91.
[82] Prasad LC, Mikula A. J Alloys Compd 1999;282:279–85.
[83] Warwick M., Implementing lead-free soldering — European Consortium Research.
[84] Suganuma K. Curr Opin Solid State Mater Sci 2001;5:55–64.
[85] Bradley III E, Hranisavljevic J. IEEE Trans Electron Packag Manuf October 2001;24–4:255–60.
[86] Chang TC, Hon MH, Chang CH, Wang MC. International Symposium of Electronic Materials and Packaging; 2001. p. 216–8.
[87] Li GY, Chen BL, Tey JN. IEEE Trans Electron Packag Manuf January 2004;27–1:77–85.
[88] Chuang CM, Shi PC, Lin KL. International Symposium on Electronic Materials and Packaging; 2002. p. 360–5.
[89] Theriault M, Blostein P. SMT; June 2000.
[90] Extrand CW. J Colloid Interface Sci 1993;157:72–6.
[91] Contreras A, Leon CA, Drew RAL, Bedolla E. Scripta Mater 2003;48: 1625–30.
[92] Yost FG. Scripta Mater 2000;42:801–6.
[93] Chidambaram PR, Edwards GR, Olson DL. Met Mat Trans B 1992;23B: 215–22.
[94] Landry K, Eustathopoulos N. Acta Mater 1996;44–10:3923–32.
[95] Eustathopoulos N, Garandet JP, Drevet B. Phil Trans R Soc Lond A 1998;356:871–84.
[96] Drevet B, Landry K, Vikner P, Eustathopoulos N. Scripta Mater 1996;35–11: 1265–70.
[97] Landry K, Kalogeropoulou S, Eustathopoulos N, Naidich Y, Krasovsky V. Scripta Mater 1996;34–6:841–6.
[98] Espie L, Drevet B, Eustathopoulos N. Met Mat Trans A 1994;25A: 599–605.
[99] Eustathopoulos N. Curr Opin Solid State Mater Sci 2005;9–4(5):152–60.
[100] Schwartz AM. Adv Colloid Interface Sci 1975;4:349–74.
[101] Coninck JD, de Ruijter MJ, Voue M. Curr Opin Colloid Interface Sci 2001;6: 49–53.
[102] Haferl S, Butty V, Poulikakos D, Giannakouros J, Boomsma K, Megaridis CM, Nayagam V. Int J Heat Mass Transfer 2001;44:3513–28.
[103] Pasandideh-Fard M, Bhola R, Chandra S, Mostaghimi J. Int J Heat Mass Transfer 1998;41:2929–45.
[104] Aziz SD, Chandra S. Int J Heat Mass Transfer 2000;43:2841–57.
[105] Haferl S, Poulikakos D. Int J Heat Mass Transfer 2003;46:535–50.
[106] Attinger D, Zhao Z, Poulikakos D. Trans ASME 2000;122:544–56.
[107] Bayer IS, Megaridis CM. XXI ICTAM; Aug. 15–21 2004.
[108] Alteraifi AM, Herbawi A. The forth annual UAE University Research Conference, STD-26 to STD-29.
[109] Starov VM, Zhdanov SA, Kosvintsev SR, Sobolev VD, Velarde MG. Adv Colloid Interface Sci 2003;104:123–58.
[110] Blake TD, Dobson RA, Ruschak KJ. J Colloid Interface Sci 2004;279: 198–205.
[111] Wyart FB, de Gennes PG. Adv Colloid Interface Sci 1992;39:1–11.
[112] Yost FG, Rye RR, Mann Jr JA. Acta Mater 1997;45–12:5337–45.
[113] Yost FG, O'toole EJ. Acta Mater 1998;46-14:5143–51.
[114] Marmur A. Adv Colloid Interface Sci 1983;19:75–102.
[115] Yost FG, Sackinger PA, O'toole EJ. Acta Mater 1998;46–7:2329–36.
[116] Vasilchina H, Tzonova I, Petrov JG. Colloids Surf A 2004;250:317–24.
[117] Gu Y, Li D. Colloids Surf A 1998;142:243–56.
[118] Erickson D, Blackmore B, Li D. Colloids Surf A 2001;182:109–22.
[119] Blake TD. J Colloid Interface Sci 2006;299–1:1–13.
[120] Seveno D. (http://thesis.ulb.ac.be:8002/ETD-db) 2004; p. 14–15.
[121] Ranabothu SR, Karnezis C, Dai LL. J Colloid Interface Sci 2005;288:213–21.
[122] Starov VM, Kalinin VV, Chen JD. Adv Colloid Interface Sci 1994;50:187–221.